Supplementary Material for
Are we ready for Autonomous Driving?

Anonymous CVPR submission

Paper ID 954

This supplementary material gives more details on our dataset, and shows additional results of the methods we have evaluated. First we present stereo and optical results, then visual odometry, and we conclude with 3D object detection and estimation.

1. Stereo and Optical Flow

For stereo and optical flow evaluation Table 1-4 provide results with additional disparity / end-point error thresholds, ranging 2 to 5 pixels. Further, Fig. 1-15 show random samples from our stereo and optical flow benchmarks:

- First row: Left, right and successive left camera image
- Second row: Disparity ground truth, estimation (SGBM) and error map (ranging $0 - 5$ pixels)
- Third row: Optical flow ground truth, estimation (Horn-Schunck) and error map (ranging $0 - 5$ pixels)

Note that for illustration purposes the depth and flow maps have been interpolated. For quantitative evaluation only pixels with associated ground truth are used. Due to the characteristics of the employed sensor, ground truth is available for approximately 30% of all pixels in the image.

2. Visual Odometry

Fig. 16-20 qualitatively compare ground truth and estimated trajectories on our visual odometry / SLAM benchmark in bird's eye perspective. Ground truth velocity profiles highlight the high variability and challenges our dataset poses to the evaluated algorithms. The enclosed file **supplementary.avi**[1] illustrates sequence 15 from our dataset, where the ground truth trajectory is shown in black and the best performing method (LIBVISO2) in blue. The red circle shows the vehicle's current position. Due to space limitations, the video has been downsampled and compressed. In our benchmark we will provide all sequences at 10 Hz with full resolution (1392×512 pixels) saved as lossless compressed png image sequences.

3. 3D Object Detection and Orientation Estimation

3D object orientation confusion matrices are presented in Fig. 21 for Histogram-of-Oriented-Gradients features and nearest neighbor, SVM and Random Forest classifiers. Fig. 22-25 further illustrate scenes from our annotated 3D object detection and orientation dataset which have been automatically retrieved.

[1]Codec: XVID MPEG-4, Recommended Video Player: VLC, available at http://www.videolan.org/vlc/

CVPR #954

Stereo Matching	Rank	Non-Occluded Pixels			All Pixels			Ø Time
		Min	Mean	Max	Min	Mean	Max	
Semiglobal BM [8]	1	**4.26** %	**14.95** %	**36.34** %	**4.82** %	**17.37** %	41.56 %	1.1 s
LIBELAS [7]	2	4.81 %	15.82 %	37.66 %	7.04 %	17.64 %	**38.95** %	0.3 s
SDM [11]	3	6.74 %	17.50 %	40.47 %	6.90 %	19.34 %	45.72 %	57.2 s
GCSF [4]	4	8.53 %	18.36 %	36.92 %	8.76 %	20.25 %	41.45 %	2.4 s
GCS [5]	5	6.78 %	19.27 %	42.22 %	6.97 %	21.15 %	46.04 %	2.2 s
Block Matching [1]	6	14.22 %	28.59 %	49.15 %	15.20 %	30.95 %	53.45 %	**0.1** s
CostFilter [12]	7	12.55 %	29.98 %	60.99 %	13.50 %	31.38 %	62.16 %	212.4 s
GC+occ [10]	8	14.45 %	41.94 %	86.41 %	16.07 %	43.59 %	86.37 %	365.9 s

Optical Flow	Rank	Non-Occluded Pixels			All Pixels			Ø Time
		Min	Mean	Max	Min	Mean	Max	
Horn Schunck [9]	1	0.01 %	**21.33** %	**75.85** %	0.01 %	**31.21** %	**82.69** %	161.6 s
Classic+NL [15]	2	**0.00** %	24.77 %	76.03 %	**0.00** %	34.51 %	82.80 %	192.3 s
LDOF [3]	3	0.06 %	24.90 %	76.70 %	0.32 %	34.84 %	83.31 %	62.3 s
Duality-based TV-L1 [17]	4	0.00 %	32.38 %	82.96 %	0.26 %	41.34 %	87.76 %	16.2 s
HAOF [2]	5	0.00 %	36.14 %	100.00 %	0.00 %	44.50 %	100.00 %	16.2 s
GCSF [4]	6	4.00 %	38.02 %	82.65 %	4.01 %	46.46 %	87.54 %	**2.4** s
Block Matching [1]	7	13.68 %	65.34 %	100.00 %	13.73 %	70.19 %	100.00 %	109.7 s
Pyramid-LK [16]	8	5.95 %	72.46 %	97.89 %	6.00 %	76.20 %	98.11 %	93.2 s

Table 1. **Stereo Matching and Optical Flow Estimation Errors** ($\tau = 2px$).

Stereo Matching	Rank	Non-Occluded Pixels			All Pixels			Ø Time
		Min	Mean	Max	Min	Mean	Max	
LIBELAS [7]	1	**1.30** %	**9.18** %	**24.64** %	2.68 %	**10.82** %	**25.51** %	0.3 s
Semiglobal BM [8]	2	1.69 %	10.89 %	31.42 %	**2.14** %	13.08 %	36.70 %	1.1 s
SDM [11]	3	3.27 %	10.94 %	35.84 %	3.31 %	12.47 %	40.93 %	57.2 s
GCSF [4]	4	3.60 %	11.14 %	31.00 %	4.20 %	12.72 %	35.42 %	2.4 s
GCS [5]	5	3.00 %	12.17 %	31.55 %	3.06 %	13.75 %	36.17 %	2.2 s
CostFilter [12]	6	4.87 %	21.25 %	53.96 %	5.42 %	22.52 %	55.16 %	212.4 s
Block Matching [1]	7	8.22 %	23.73 %	44.92 %	9.17 %	25.96 %	50.64 %	**0.1** s
GC+occ [10]	8	7.32 %	33.63 %	82.24 %	8.77 %	35.33 %	82.11 %	365.9 s

Optical Flow	Rank	Non-Occluded Pixels			All Pixels			Ø Time
		Min	Mean	Max	Min	Mean	Max	
Horn Schunck [9]	1	**0.00** %	**18.66** %	71.72 %	**0.00** %	**28.33** %	79.71 %	161.6 s
LDOF [3]	2	0.00 %	21.41 %	**70.51** %	0.00 %	31.45 %	**78.84** %	62.3 s
Classic+NL [15]	3	0.00 %	22.85 %	74.51 %	0.00 %	32.39 %	81.69 %	192.3 s
Duality-based TV-L1 [17]	4	0.00 %	29.02 %	78.69 %	0.14 %	38.25 %	84.68 %	16.2 s
GCSF [4]	5	2.80 %	31.47 %	77.49 %	2.83 %	40.79 %	83.79 %	**2.4** s
HAOF [2]	6	0.00 %	33.56 %	100.00 %	0.00 %	41.99 %	100.00 %	16.2 s
Block Matching [1]	7	9.33 %	62.91 %	100.00 %	9.38 %	68.10 %	100.00 %	109.7 s
Pyramid-LK [16]	8	3.10 %	65.34 %	96.41 %	3.14 %	70.10 %	96.79 %	93.2 s

Table 2. **Stereo Matching and Optical Flow Estimation Errors** ($\tau = 3px$).

Stereo Matching	Rank	Non-Occluded Pixels			All Pixels			Ø Time
		Min	Mean	Max	Min	Mean	Max	
LIBELAS [7]	1	**0.57** %	**6.34** %	**18.84** %	1.53 %	**7.81** %	**23.23** %	0.3 s
GCSF [4]	2	1.70 %	7.73 %	28.23 %	2.46 %	9.06 %	32.42 %	2.4 s
SDM [11]	3	2.07 %	7.91 %	33.63 %	2.08 %	9.18 %	38.47 %	57.2 s
GCS [5]	4	1.83 %	8.80 %	28.85 %	1.85 %	10.13 %	33.24 %	2.2 s
Semiglobal BM [8]	5	0.97 %	9.04 %	28.75 %	**1.50** %	11.05 %	33.89 %	1.1 s
CostFilter [12]	6	2.73 %	17.14 %	50.28 %	3.06 %	18.23 %	51.49 %	212.4 s
Block Matching [1]	7	5.01 %	21.71 %	43.39 %	5.83 %	23.78 %	48.98 %	**0.1** s
GC+occ [10]	8	5.53 %	29.01 %	78.79 %	6.61 %	30.72 %	78.64 %	365.9 s

Optical Flow	Rank	Non-Occluded Pixels			All Pixels			Ø Time
		Min	Mean	Max	Min	Mean	Max	
Horn Schunck [9]	1	**0.00** %	**17.27** %	68.79 %	**0.00** %	**26.62** %	77.58 %	161.6 s
LDOF [3]	2	0.00 %	19.37 %	**65.13** %	0.00 %	29.34 %	**74.94** %	62.3 s
Classic+NL [15]	3	0.00 %	21.78 %	73.48 %	0.00 %	31.08 %	80.93 %	192.3 s
Duality-based TV-L1 [17]	4	0.00 %	26.68 %	75.96 %	0.08 %	36.01 %	82.68 %	16.2 s
GCSF [4]	5	1.71 %	27.49 %	73.58 %	1.73 %	37.31 %	80.96 %	**2.4** s
HAOF [2]	6	0.00 %	31.77 %	100.00 %	0.00 %	40.18 %	100.00 %	16.2 s
Pyramid-LK [16]	7	1.83 %	60.36 %	94.93 %	1.87 %	65.85 %	95.47 %	93.2 s
Block Matching [1]	8	6.70 %	61.18 %	100.00 %	6.72 %	66.59 %	100.00 %	109.7 s

Table 3. **Stereo Matching and Optical Flow Estimation Errors** ($\tau = 4px$).

Stereo Matching	Rank	Non-Occluded Pixels			All Pixels			Ø Time
		Min	Mean	Max	Min	Mean	Max	
LIBELAS [7]	1	0.40 %	**4.96** %	**17.34** %	1.14 %	**6.28** %	**21.76** %	0.3 s
GCSF [4]	2	1.10 %	5.98 %	26.26 %	1.38 %	7.14 %	30.15 %	2.4 s
SDM [11]	3	1.24 %	6.35 %	31.82 %	1.34 %	7.45 %	36.37 %	57.2 s
GCS [5]	4	1.01 %	7.04 %	26.97 %	1.21 %	8.20 %	31.00 %	2.2 s
Semiglobal BM [8]	5	**0.29** %	7.88 %	26.96 %	**0.91** %	9.75 %	31.97 %	1.1 s
CostFilter [12]	6	1.10 %	15.16 %	48.12 %	1.60 %	16.11 %	49.30 %	212.4 s
Block Matching [1]	7	4.13 %	20.63 %	42.36 %	4.89 %	22.53 %	47.62 %	**0.1** s
GC+occ [10]	8	3.09 %	26.21 %	75.73 %	4.14 %	27.88 %	75.68 %	365.9 s

Optical Flow	Rank	Non-Occluded Pixels			All Pixels			Ø Time
		Min	Mean	Max	Min	Mean	Max	
Horn Schunck [9]	1	**0.00** %	**16.28** %	67.00 %	**0.00** %	**25.35** %	76.27 %	161.6 s
LDOF [3]	2	0.00 %	17.89 %	**60.70** %	0.00 %	27.72 %	**71.75** %	62.3 s
Classic+NL [15]	3	0.00 %	20.99 %	72.56 %	0.00 %	30.09 %	80.26 %	192.3 s
GCSF [4]	4	1.05 %	24.50 %	70.07 %	1.07 %	34.68 %	78.41 %	**2.4** s
Duality-based TV-L1 [17]	5	0.00 %	24.80 %	74.02 %	0.00 %	34.17 %	81.27 %	16.2 s
HAOF [2]	6	0.00 %	30.29 %	100.00 %	0.00 %	38.67 %	100.00 %	16.2 s
Pyramid-LK [16]	7	1.07 %	56.45 %	93.42 %	1.10 %	62.49 %	94.12 %	93.2 s
Block Matching [1]	8	4.86 %	59.68 %	100.00 %	5.06 %	65.29 %	100.00 %	109.7 s

Table 4. **Stereo Matching and Optical Flow Estimation Errors** ($\tau = 5px$).

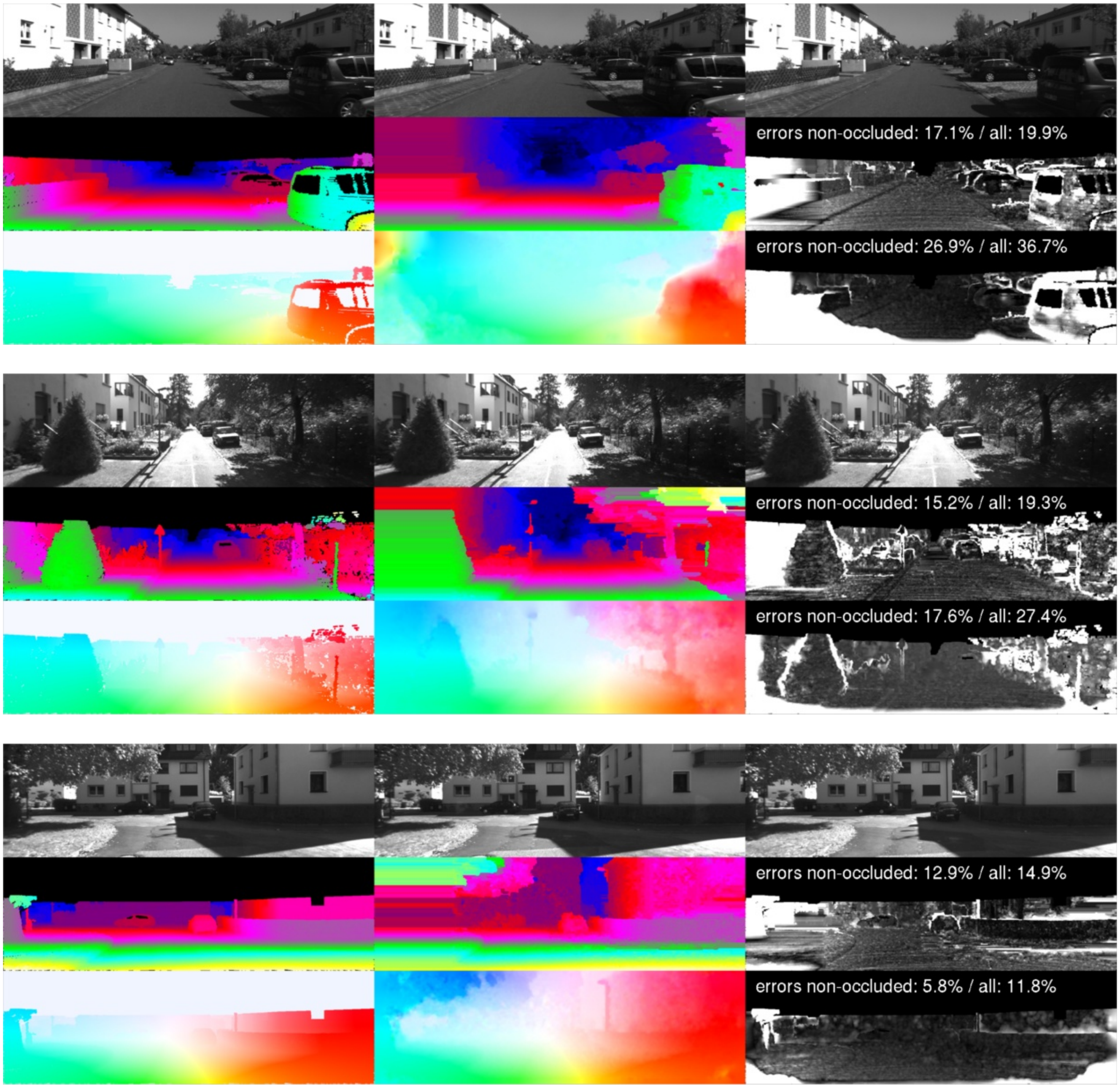

Figure 1. **Stereo and Optical Flow Dataset**

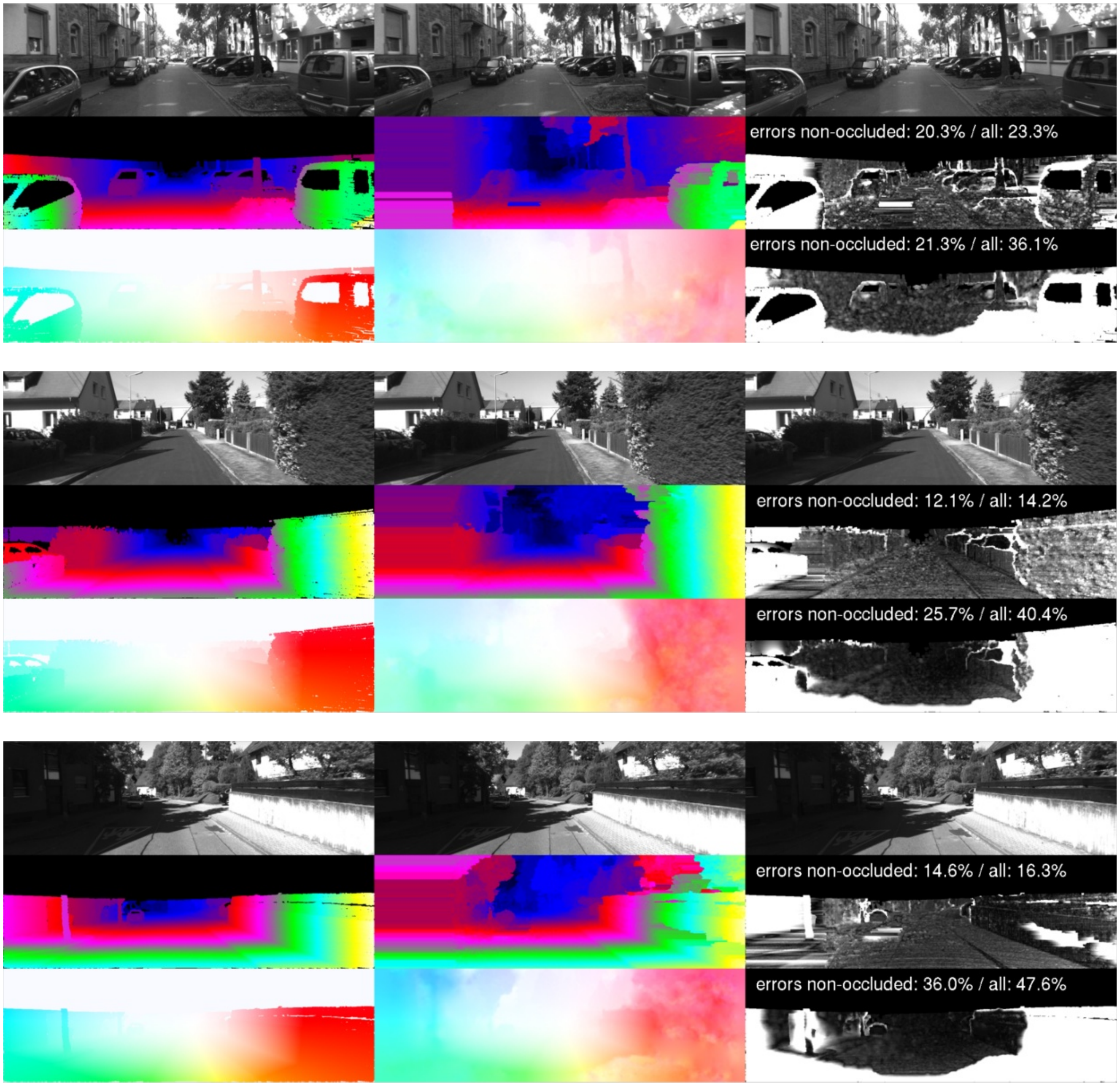

Figure 2. **Stereo and Optical Flow Dataset**

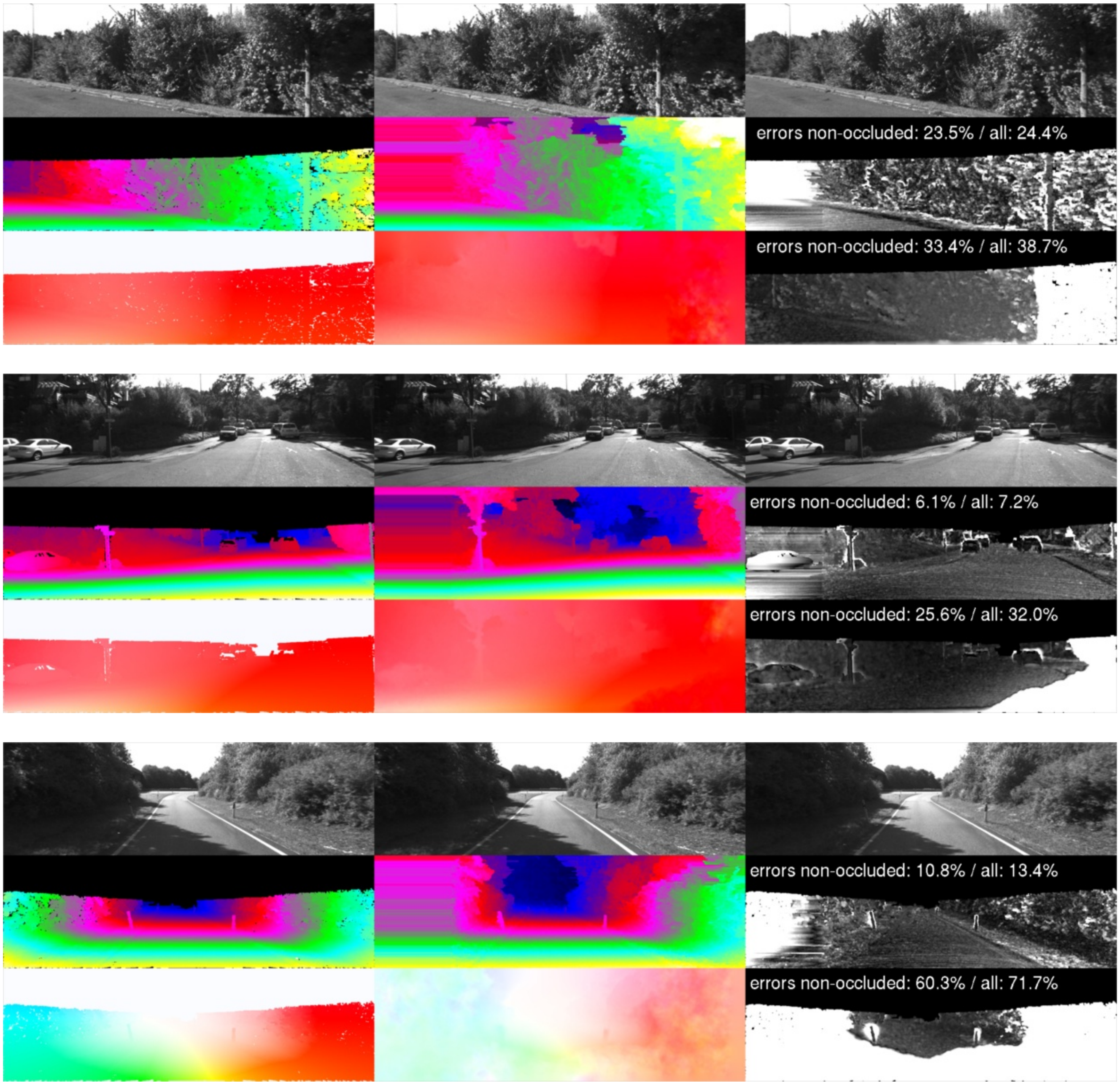

Figure 3. **Stereo and Optical Flow Dataset**

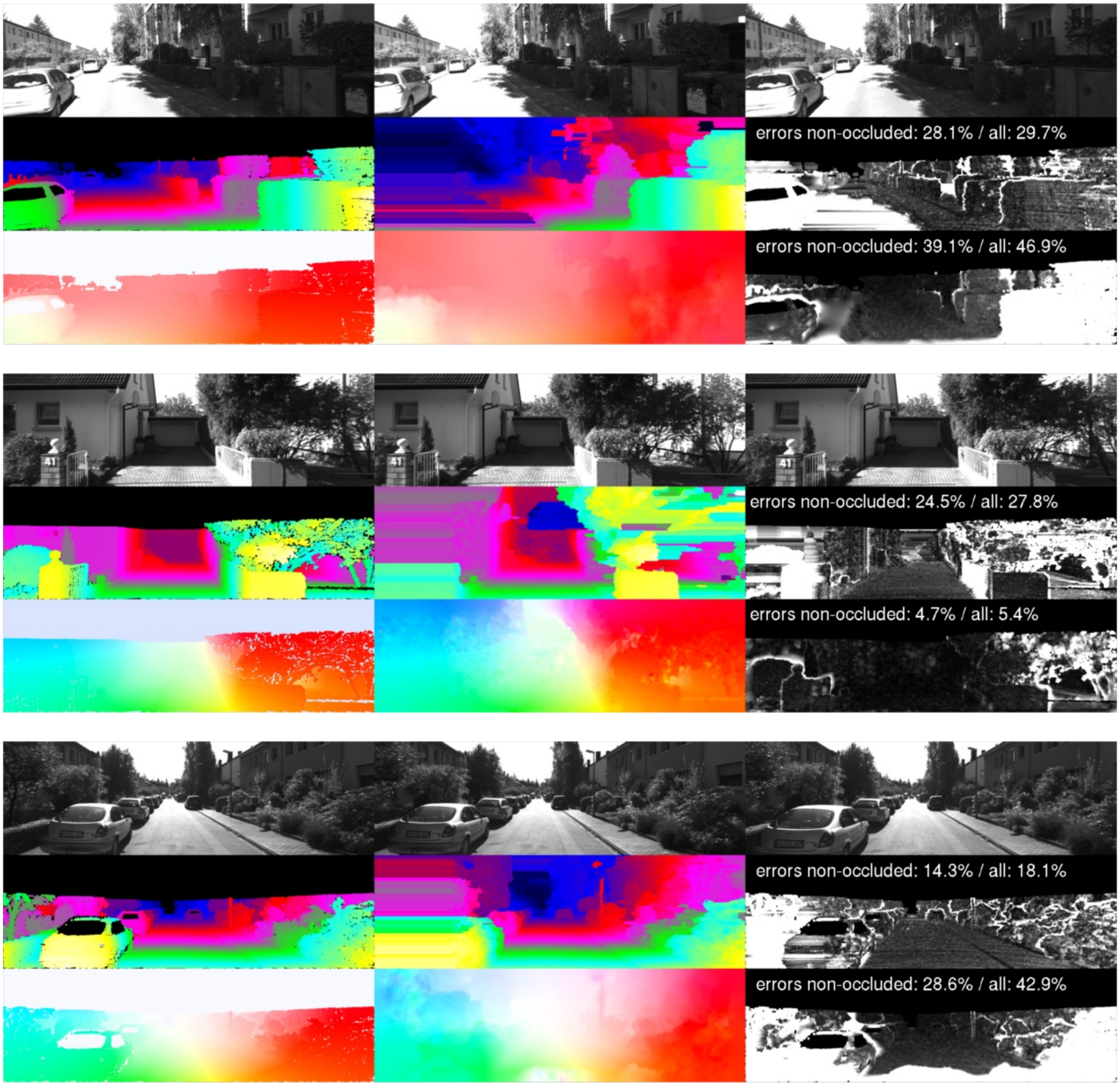

Figure 4. **Stereo and Optical Flow Dataset**

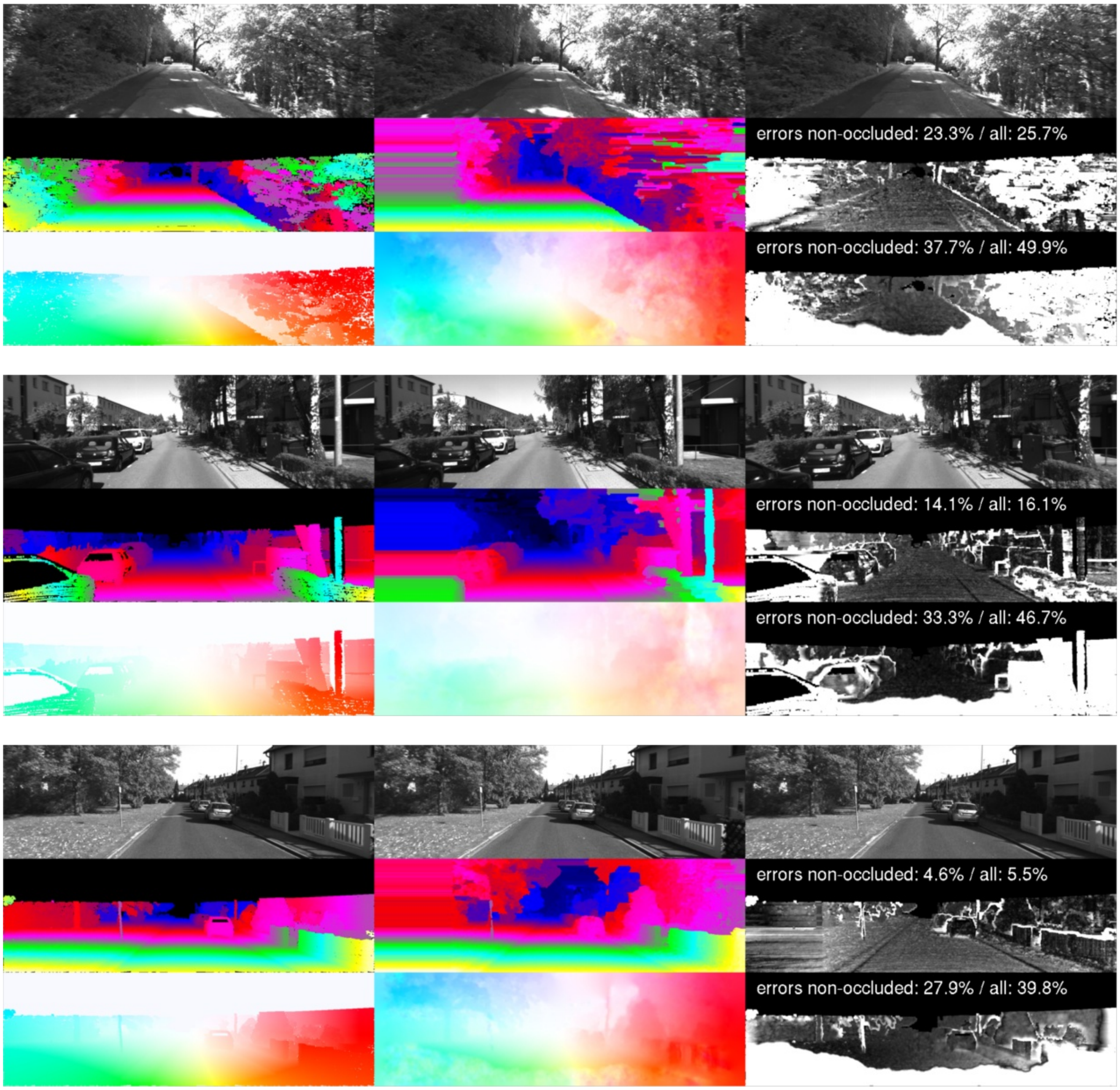

Figure 5. **Stereo and Optical Flow Dataset**

CVPR
#954

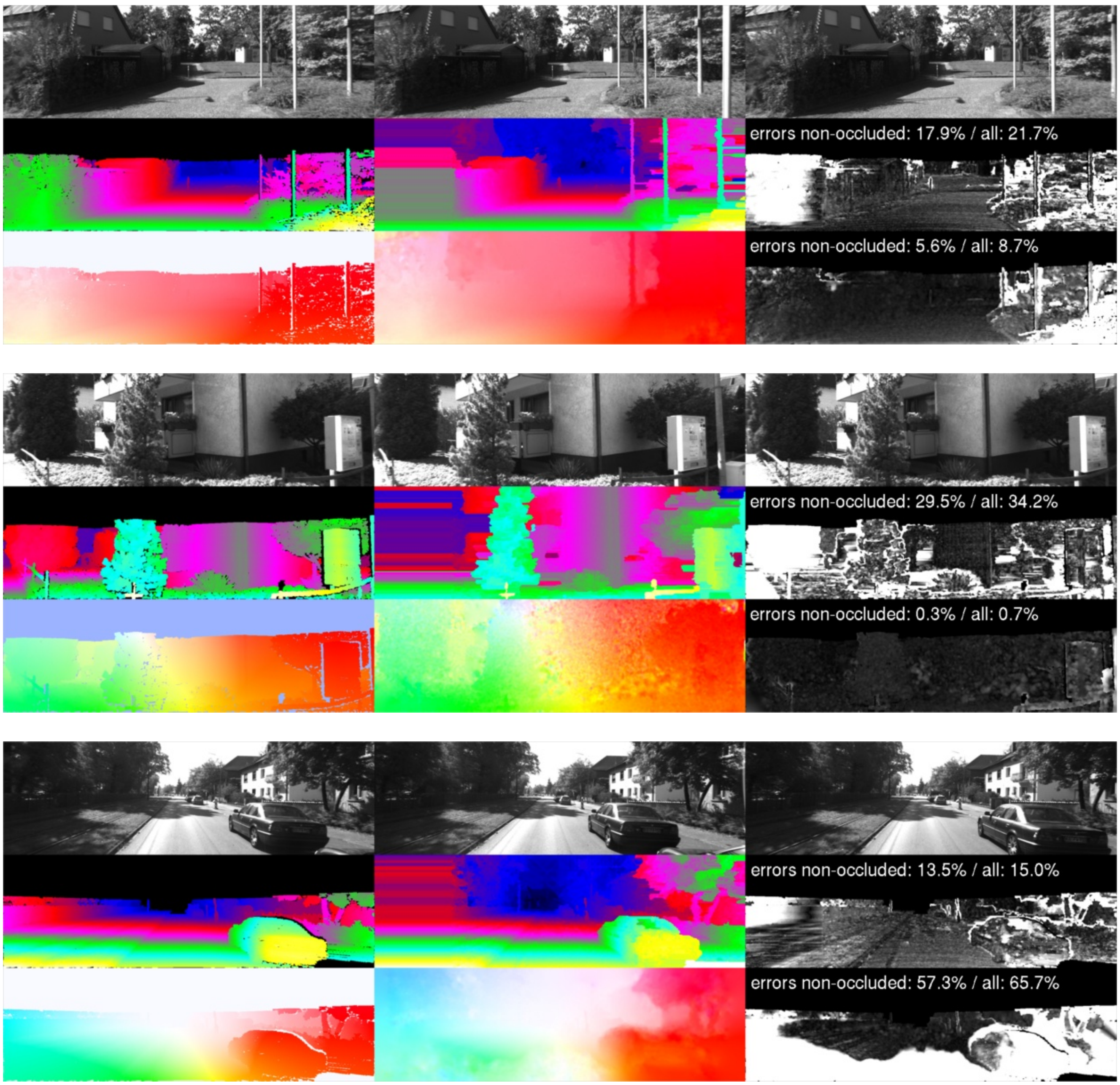

Figure 6. **Stereo and Optical Flow Dataset**

CVPR
#954

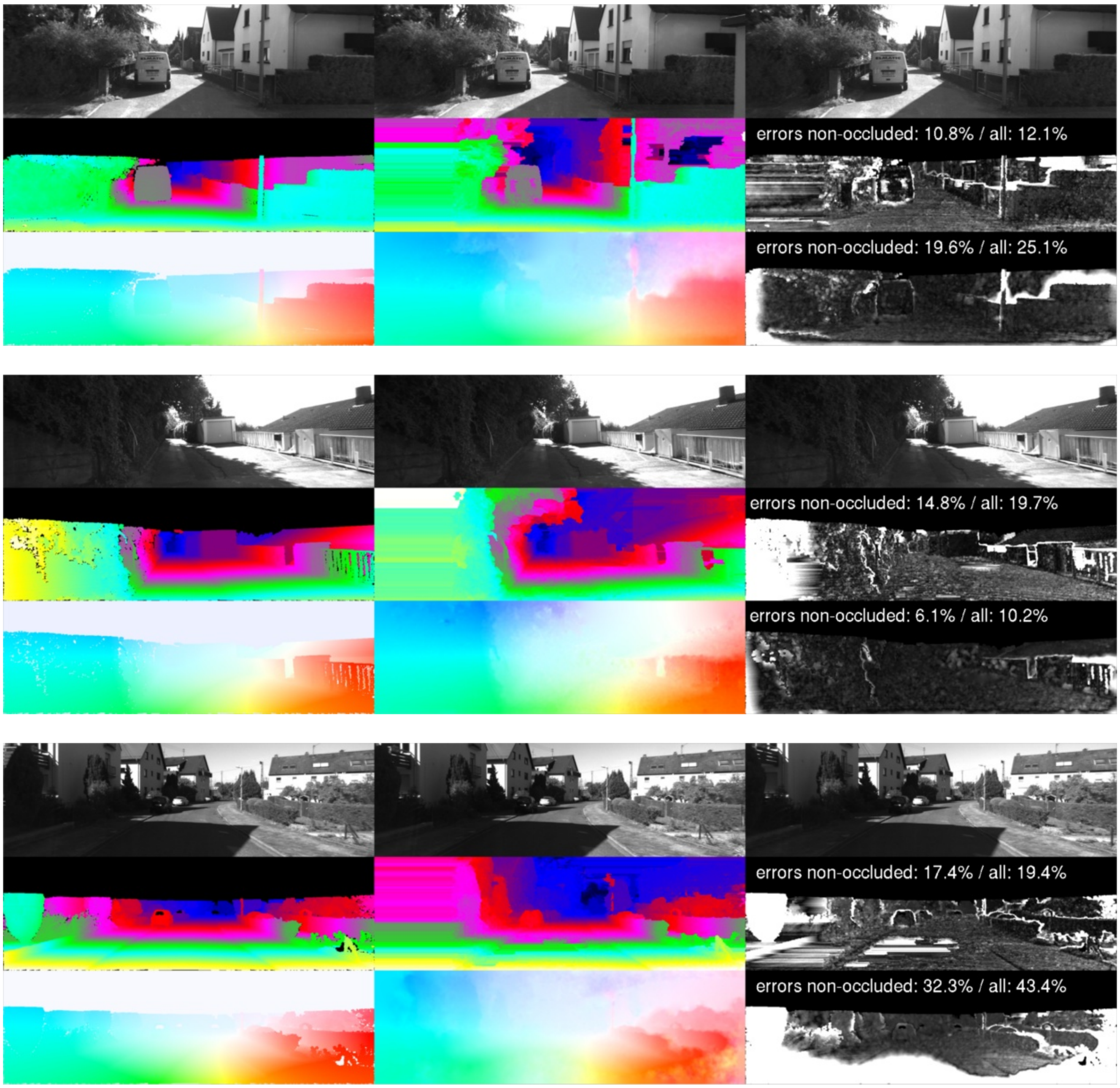

Figure 7. **Stereo and Optical Flow Dataset**

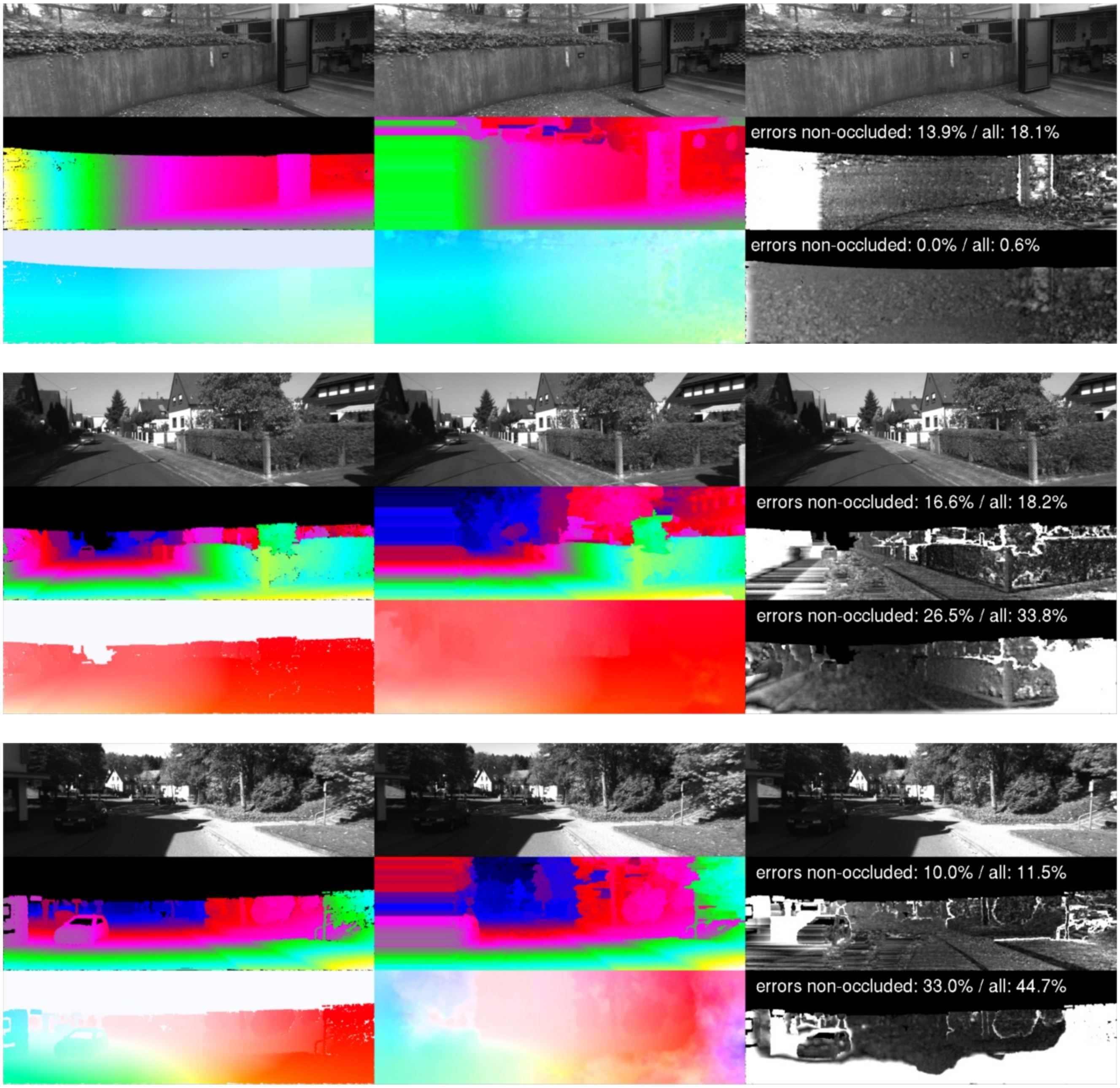

Figure 8. **Stereo and Optical Flow Dataset**

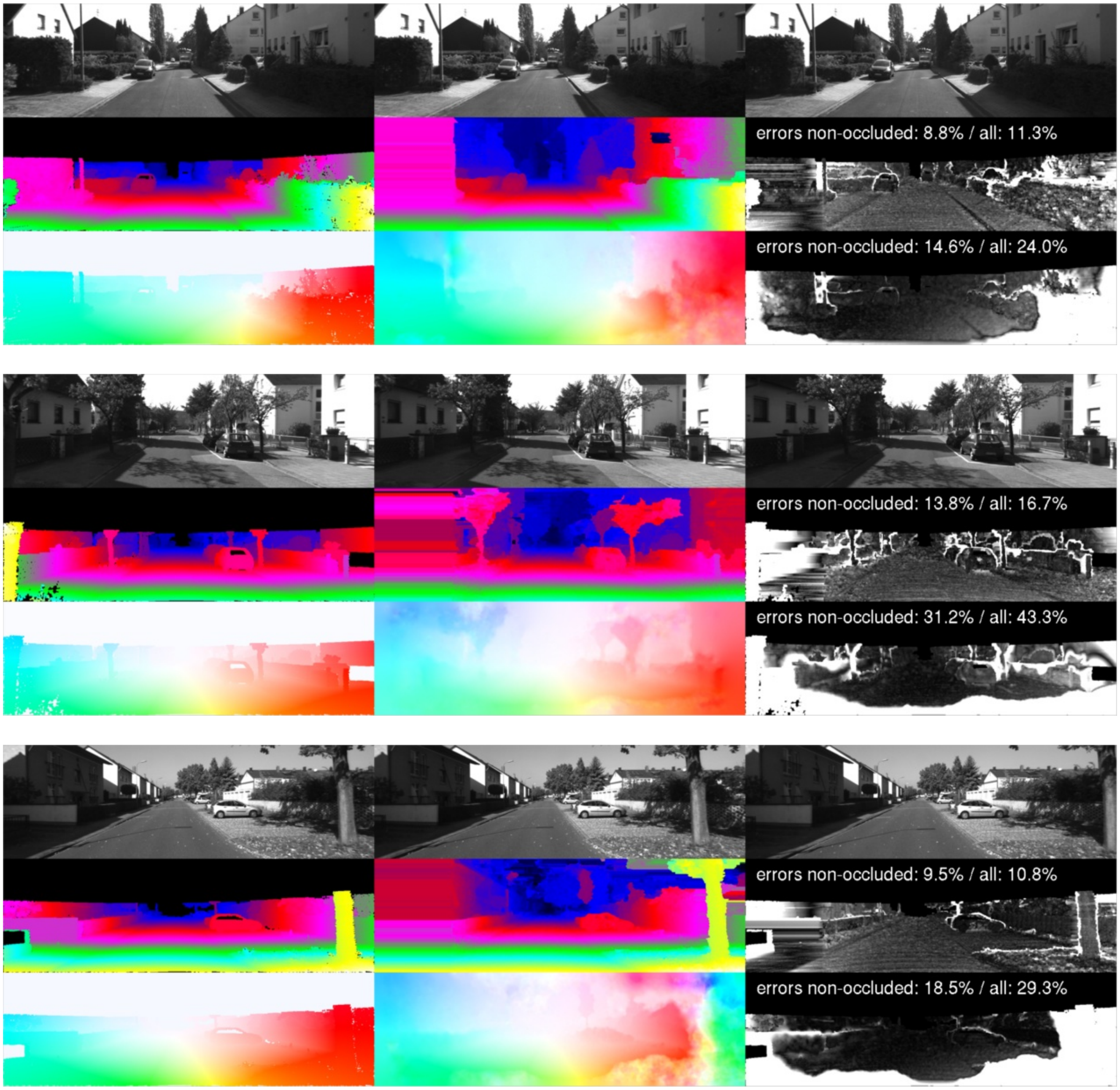

Figure 9. **Stereo and Optical Flow Dataset**

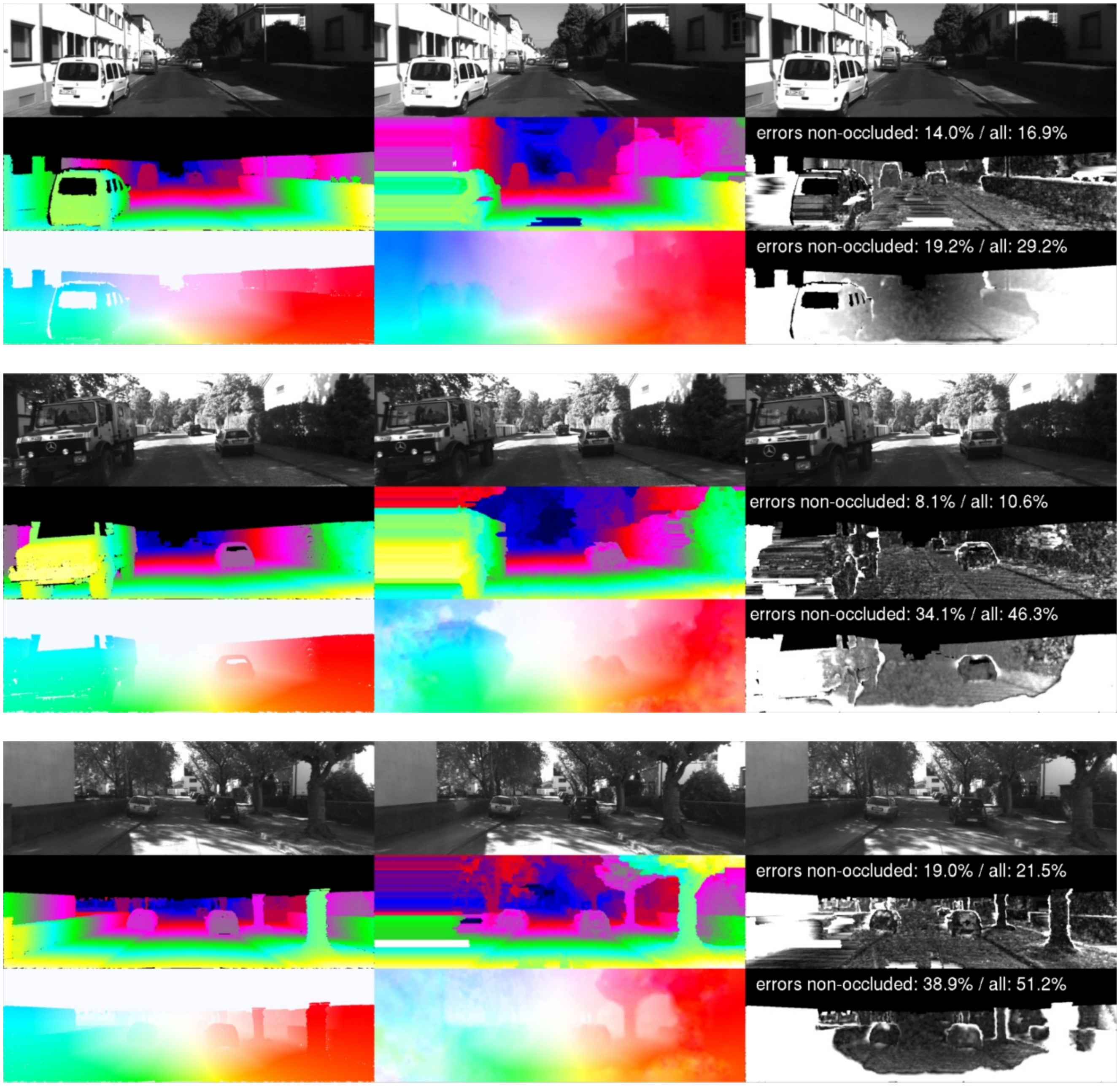

Figure 10. **Stereo and Optical Flow Dataset**

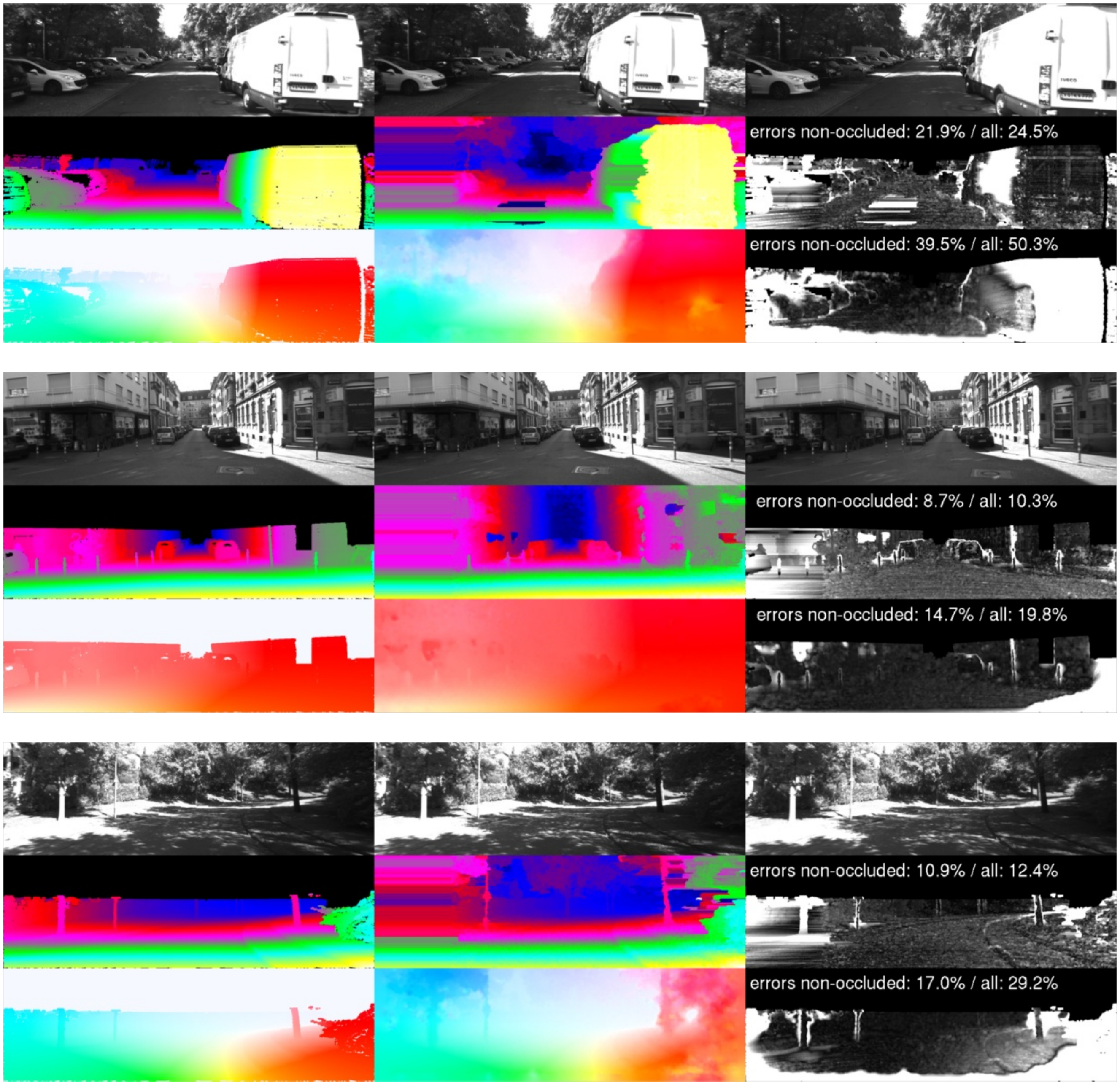

Figure 11. **Stereo and Optical Flow Dataset**

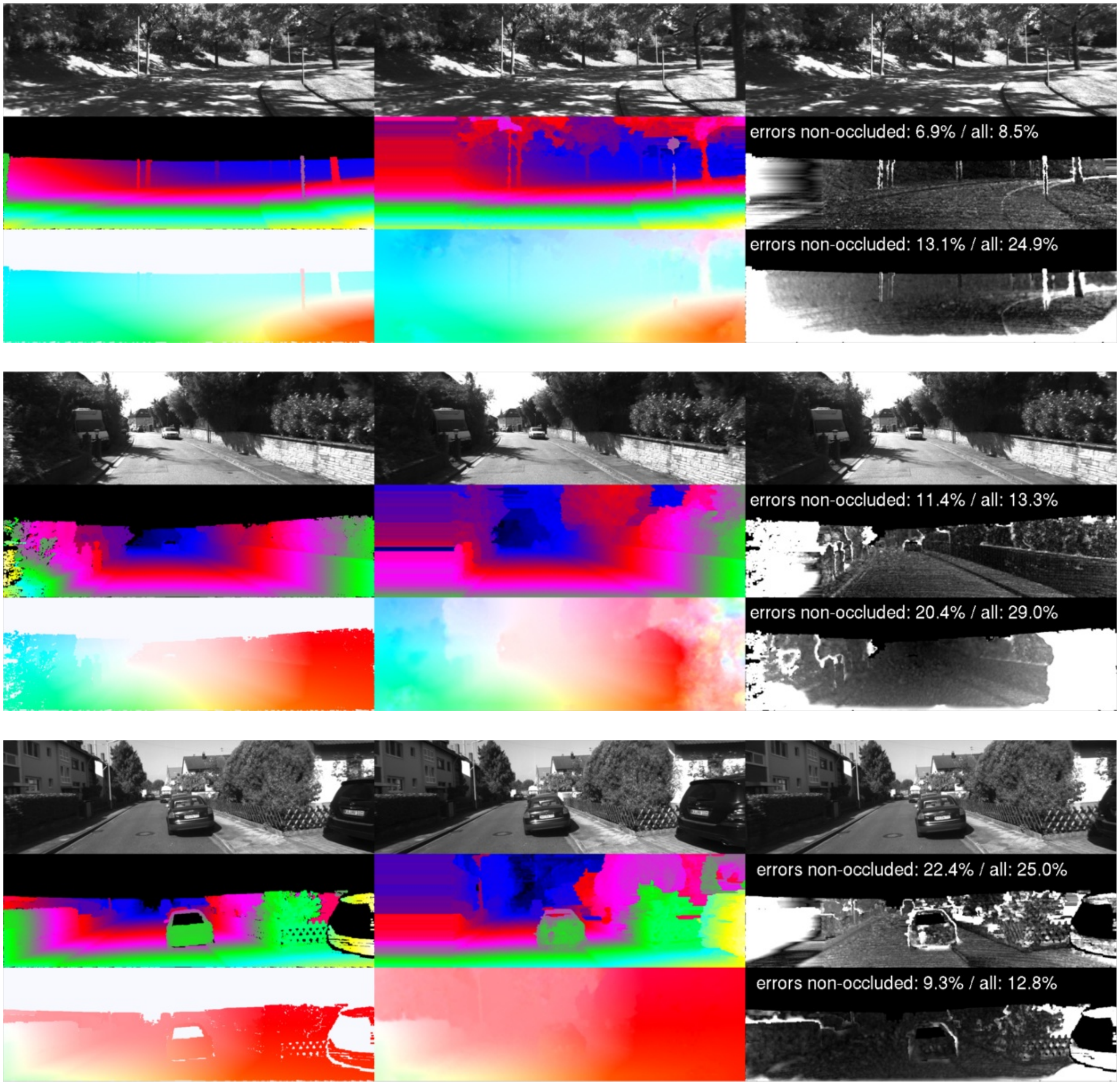

Figure 12. **Stereo and Optical Flow Dataset**

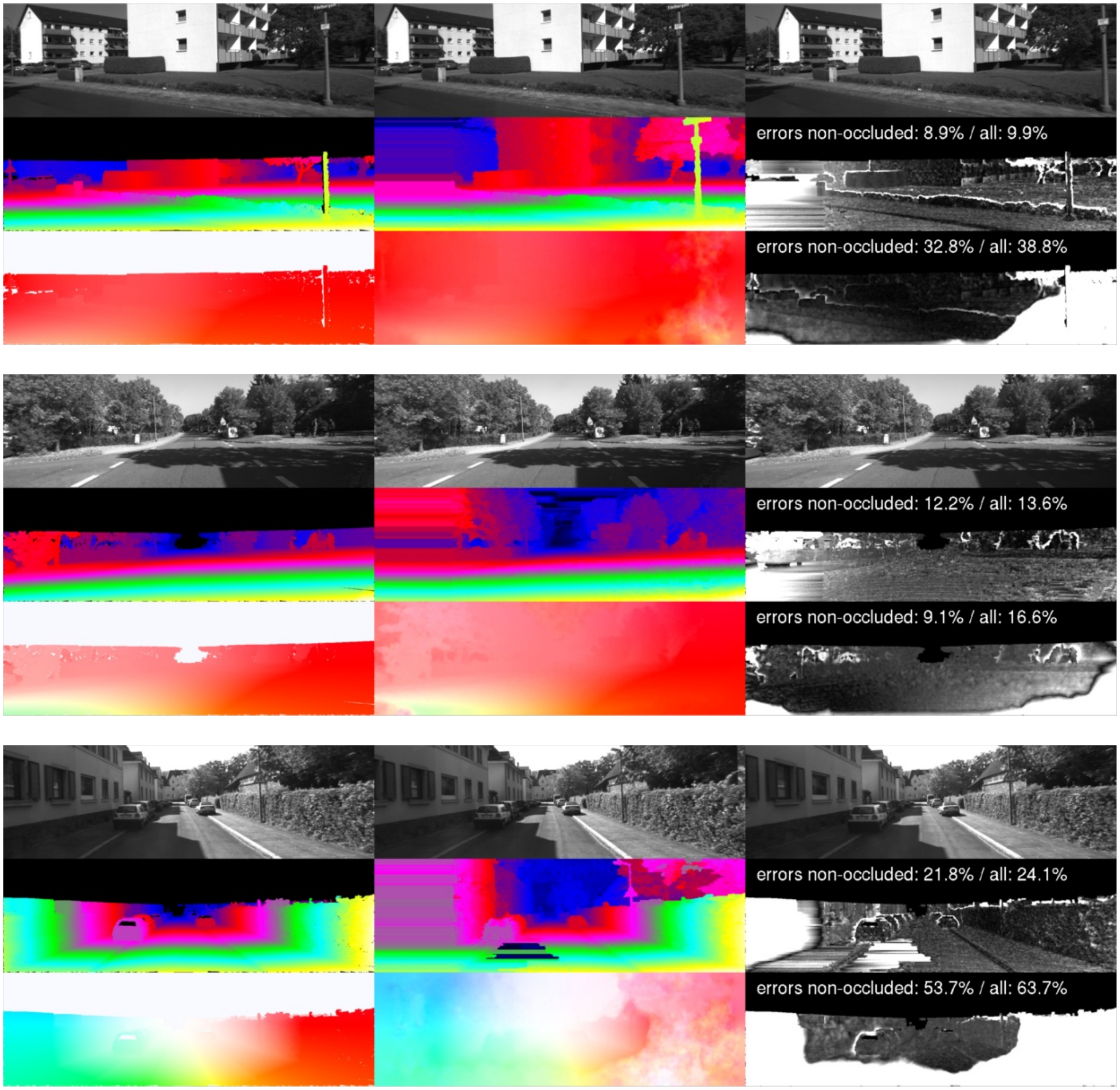

Figure 13. **Stereo and Optical Flow Dataset**

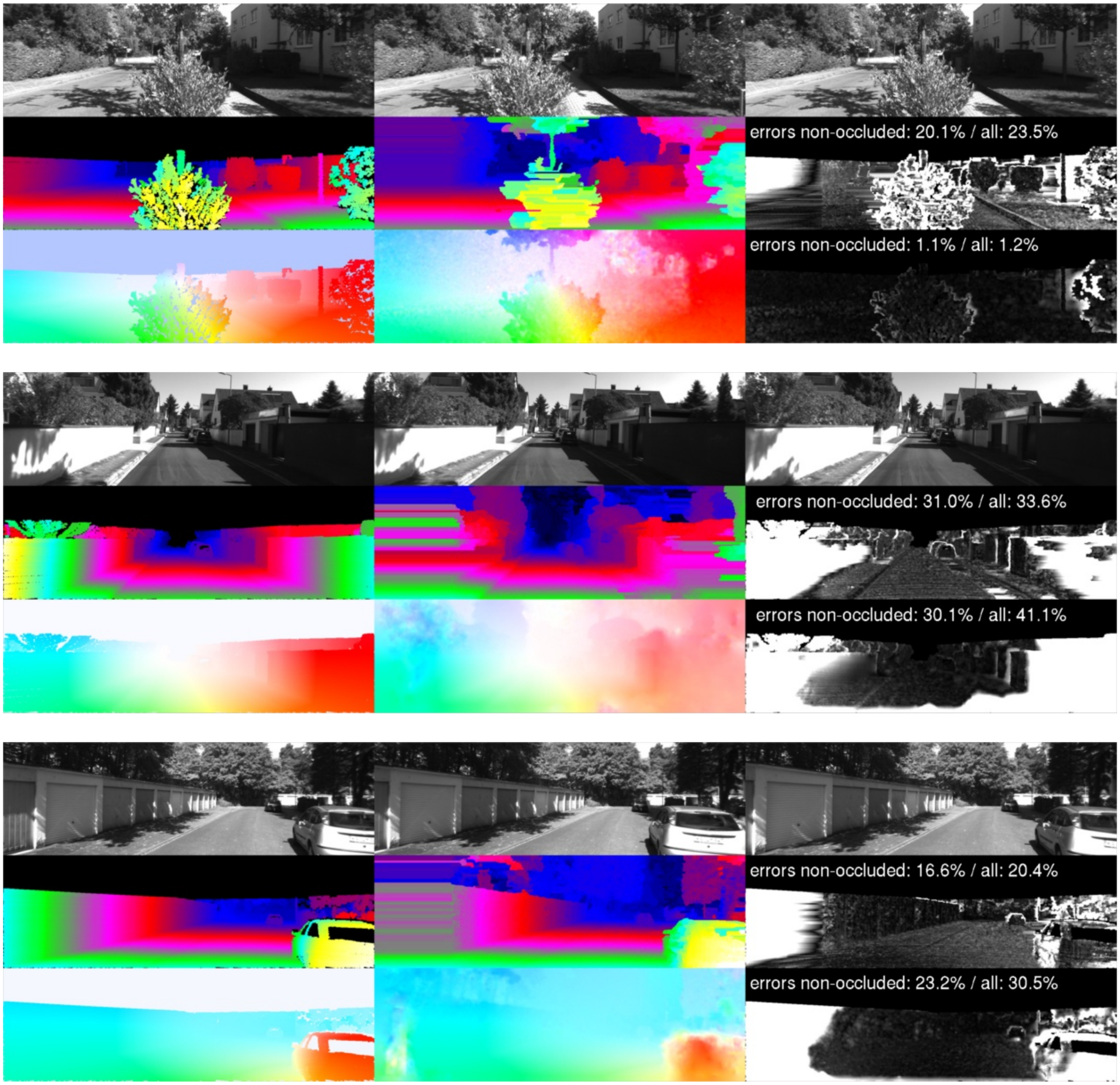

Figure 14. **Stereo and Optical Flow Dataset**

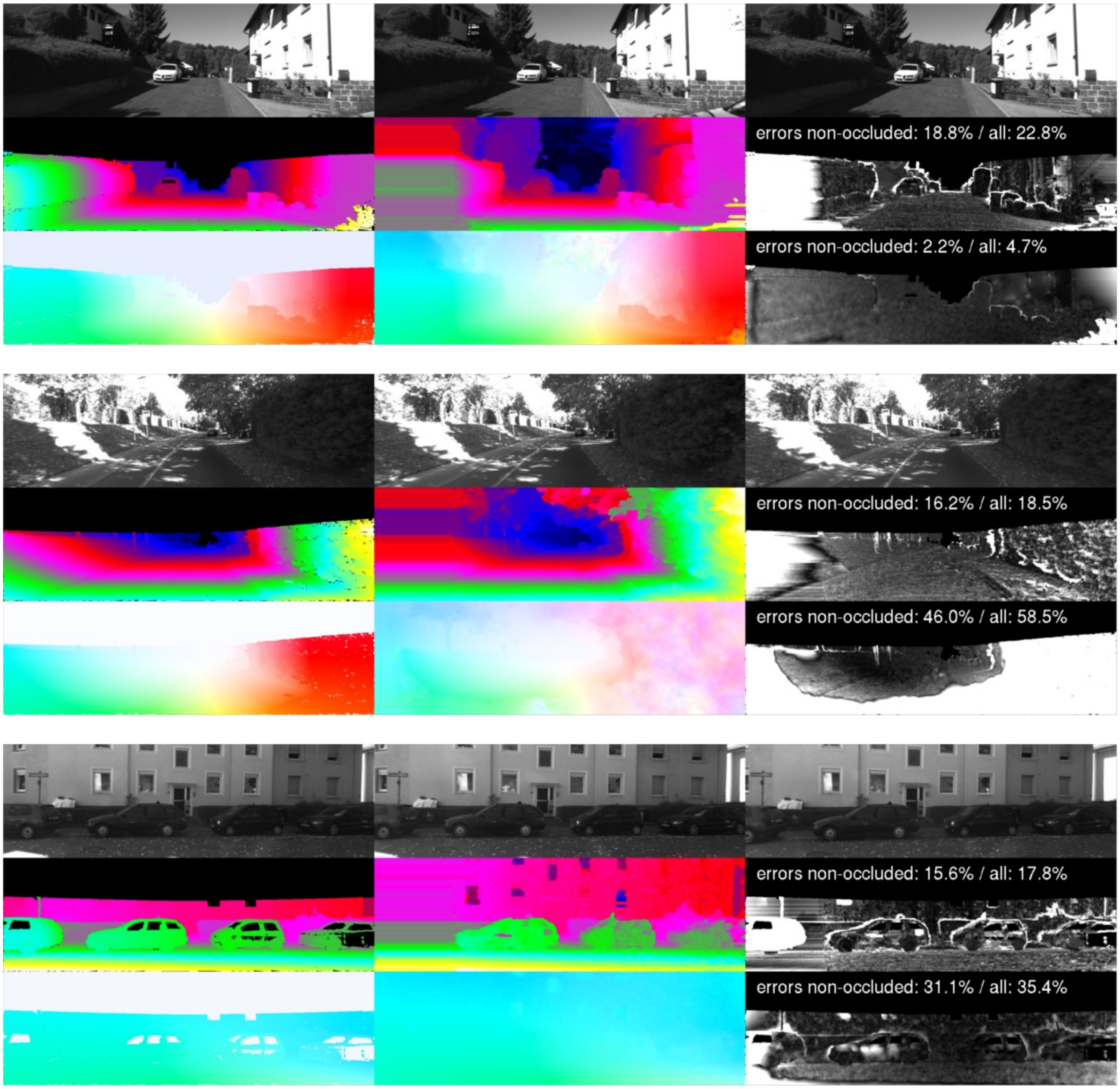

Figure 15. **Stereo and Optical Flow Dataset**

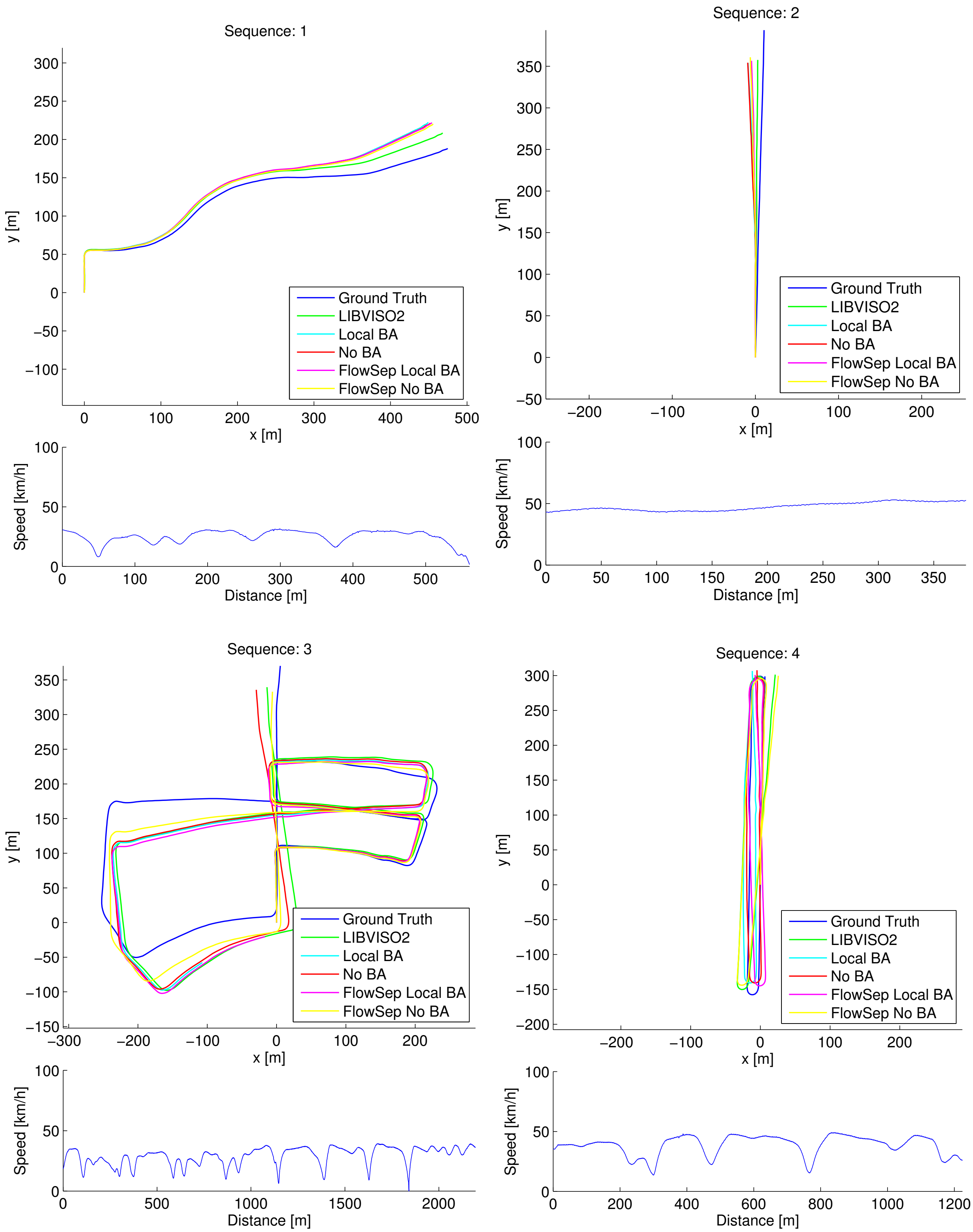

Figure 16. **Visual Odometry: Ground Truth, Estimated Trajectories and Speed Profile**

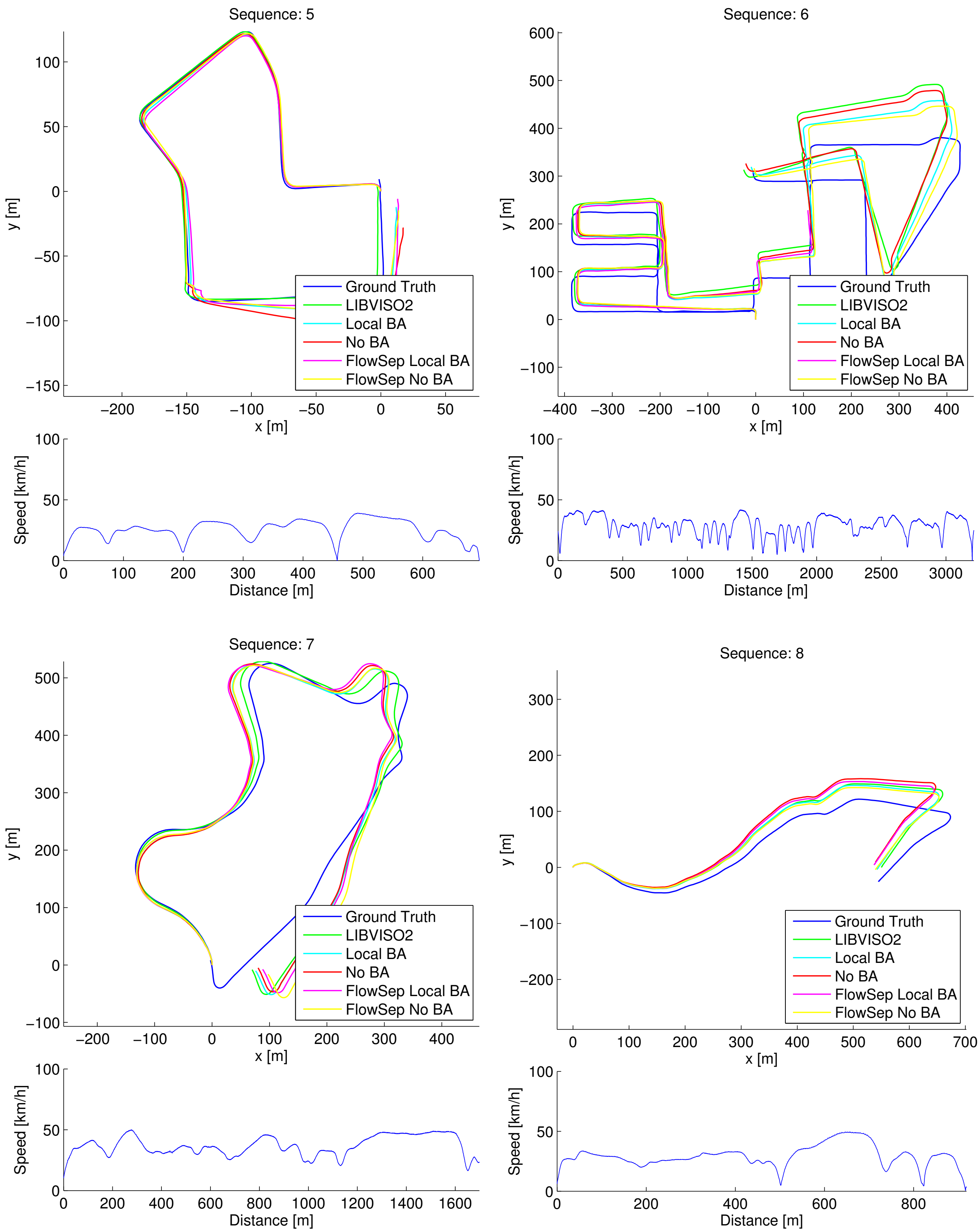

Figure 17. **Visual Odometry: Ground Truth, Estimated Trajectories and Speed Profile**

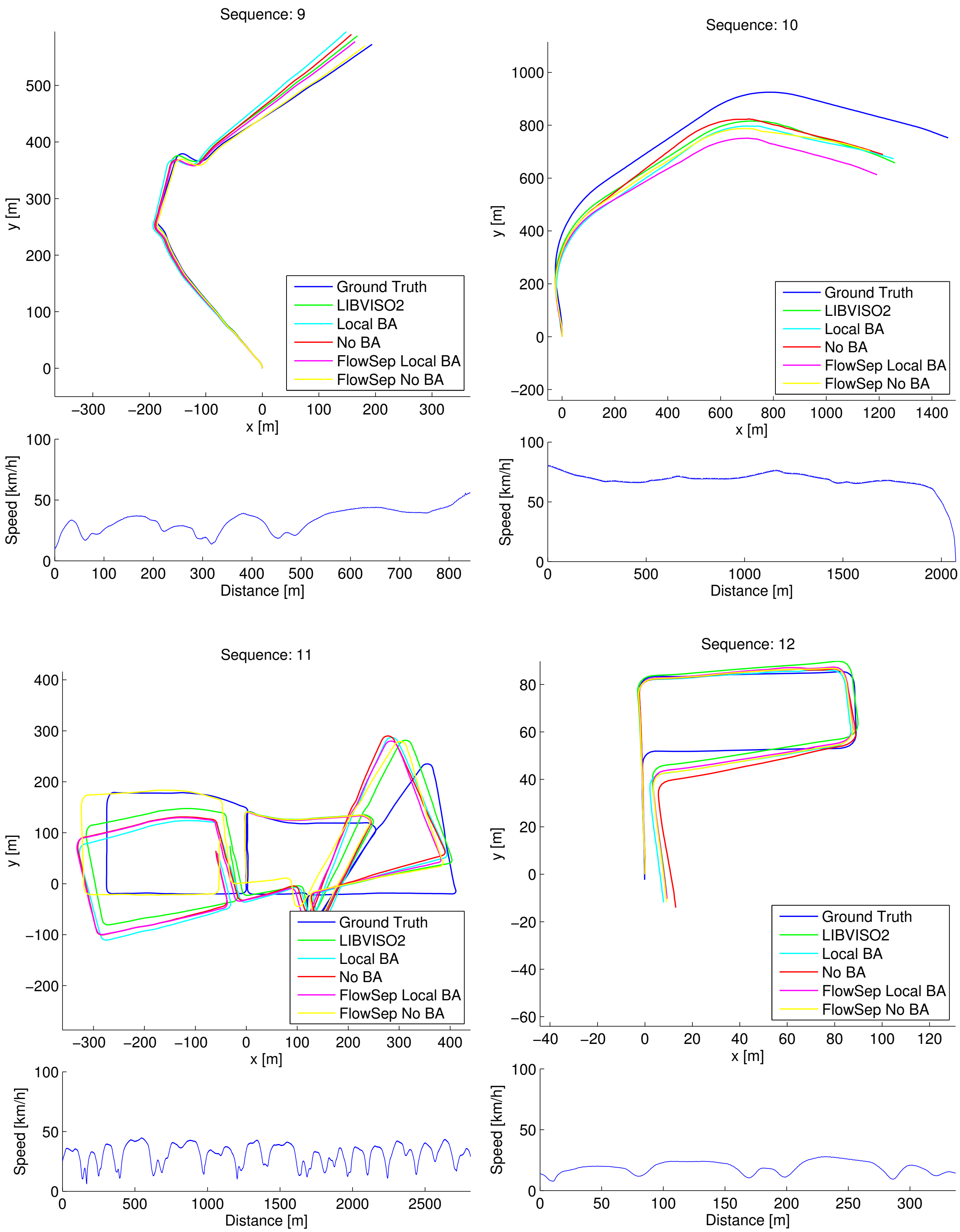

Figure 18. **Visual Odometry: Ground Truth, Estimated Trajectories and Speed Profile**

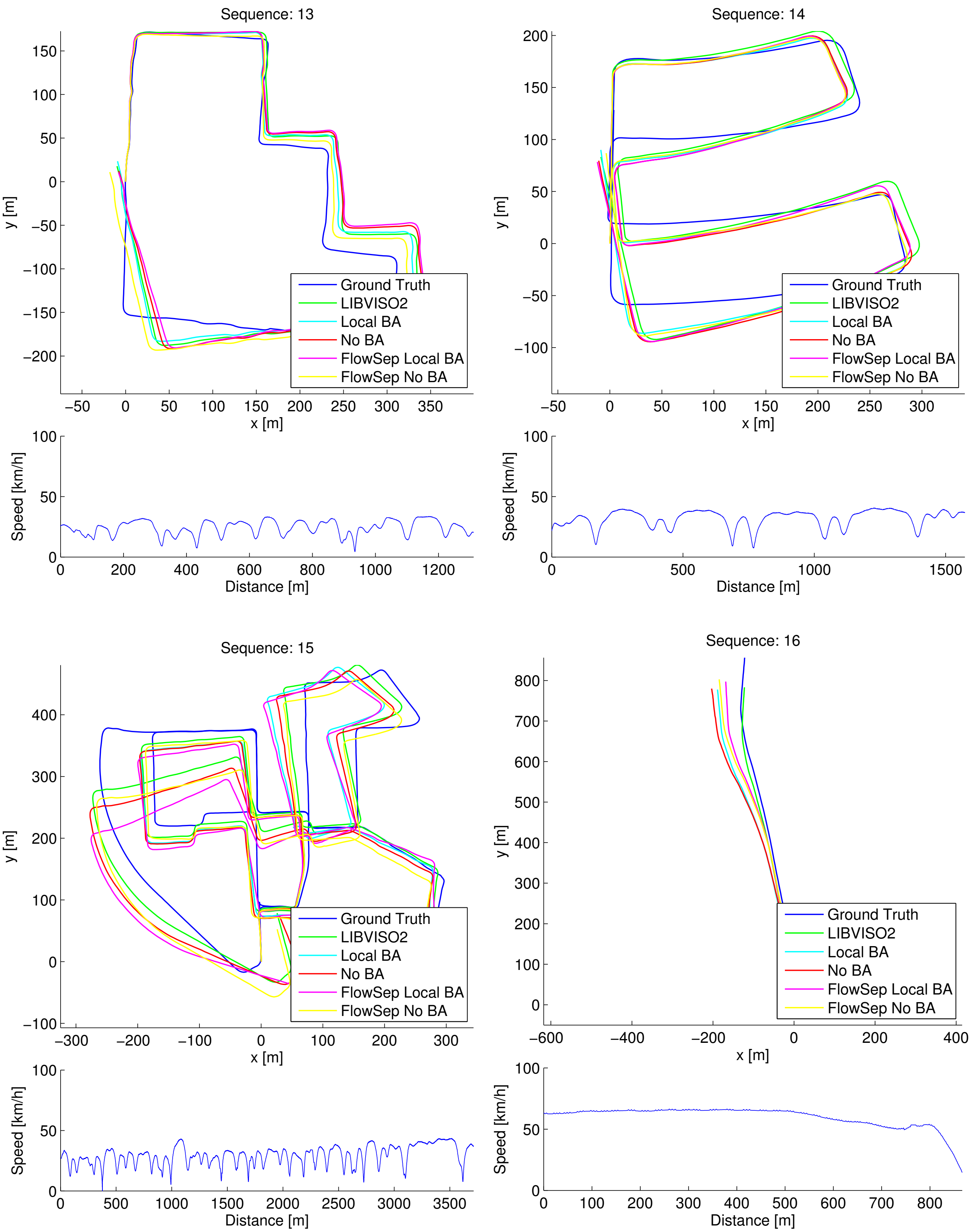

Figure 19. **Visual Odometry: Ground Truth, Estimated Trajectories and Speed Profile**

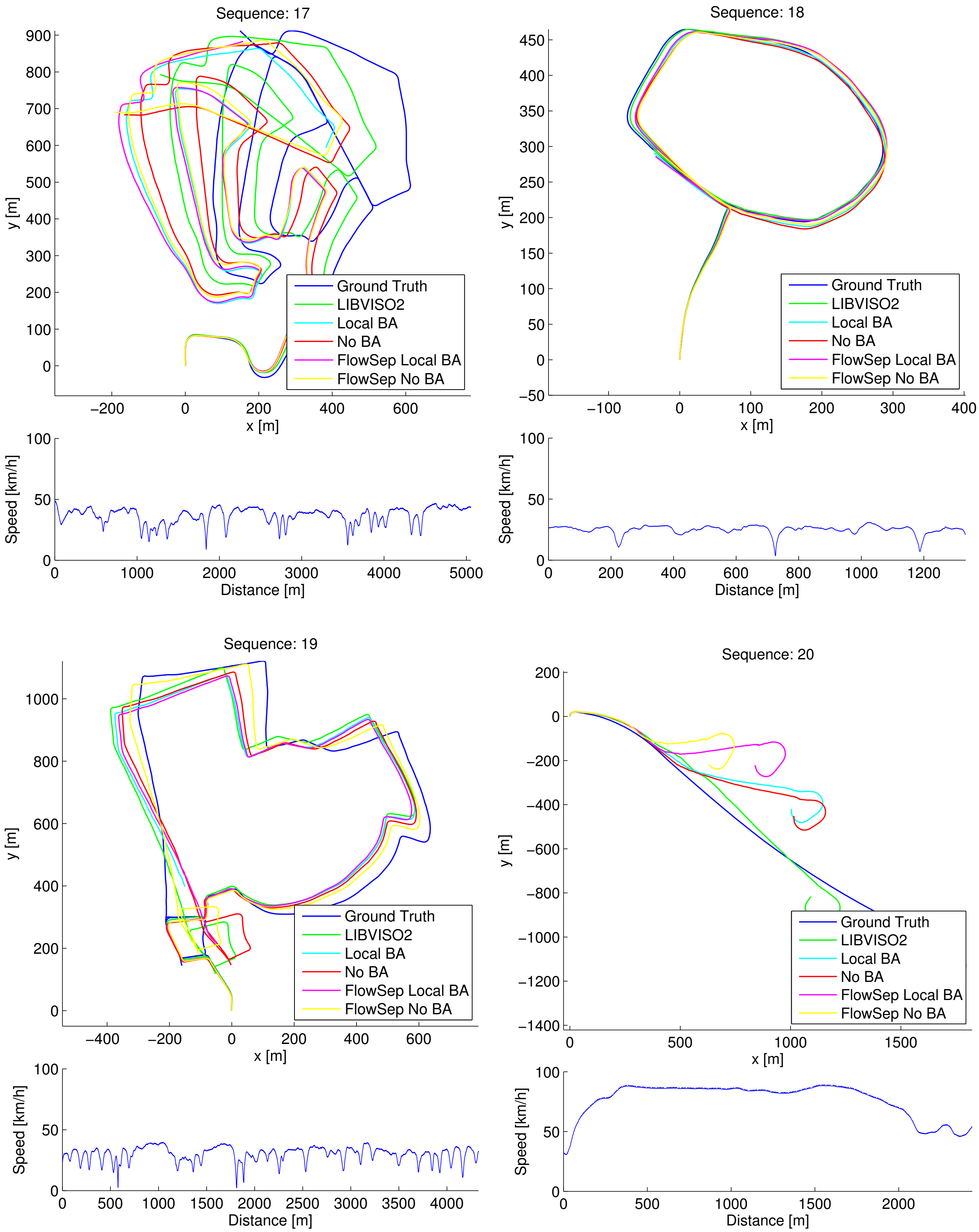

Figure 20. **Visual Odometry: Ground Truth, Estimated Trajectories and Speed Profile**

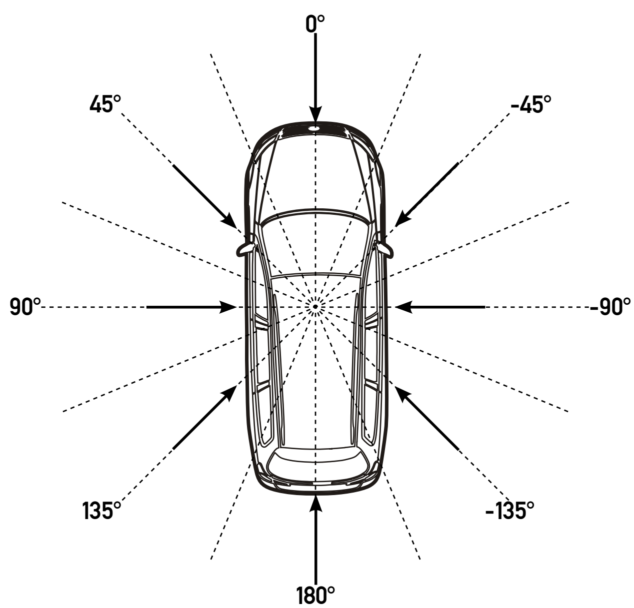

(a) **16 Object Orientations used for Classification**

True Orientation [deg]	-157.5	-135.0	-112.5	-90.0	-67.5	-45.0	-22.5	-0.0	22.5	45.0	67.5	90.0	112.5	135.0	157.5	180.0
-157.5	59.0	12.8	0.0	0.0	0.0	0.0	0.0	5.1	5.1	0.0	0.0	0.0	5.1	5.1	0.0	7.7
-135.0	4.0	44.0	20.0	0.0	4.0	0.0	4.0	0.0	0.0	12.0	8.0	0.0	4.0	0.0	0.0	0.0
-112.5	0.0	3.6	82.1	3.6	3.6	0.0	7.1	0.0	0.0	0.0	0.0	0.0	0.0	0.0	0.0	0.0
-90.0	0.0	7.7	38.5	15.4	30.8	0.0	7.7	0.0	0.0	0.0	0.0	0.0	0.0	0.0	0.0	0.0
-67.5	0.0	0.0	5.6	22.2	55.6	5.6	0.0	0.0	0.0	0.0	0.0	0.0	5.6	5.6	0.0	0.0
-45.0	0.0	0.0	14.3	0.0	50.0	21.4	14.3	0.0	0.0	0.0	0.0	0.0	0.0	0.0	0.0	0.0
-22.5	0.0	0.0	5.3	0.0	0.0	0.0	78.9	5.3	0.0	0.0	0.0	0.0	0.0	5.3	5.3	0.0
-0.0	2.0	0.0	0.0	0.0	0.0	0.0	2.0	82.0	12.0	0.0	0.0	0.0	2.0	0.0	0.0	0.0
22.5	0.0	0.0	0.0	0.0	0.0	0.0	0.0	12.2	59.2	22.4	2.0	0.0	2.0	2.0	0.0	0.0
45.0	0.0	0.0	0.0	0.0	0.0	0.0	0.0	2.6	7.7	71.8	15.4	2.6	0.0	0.0	0.0	0.0
67.5	0.0	4.0	4.0	0.0	0.0	0.0	0.0	0.0	0.0	16.0	44.0	28.0	4.0	0.0	0.0	0.0
90.0	0.0	0.0	0.0	0.0	0.0	0.0	0.0	0.0	0.0	0.0	45.0	25.0	25.0	5.0	0.0	0.0
112.5	0.0	0.0	0.0	0.0	0.0	0.0	0.0	0.0	0.0	0.0	3.8	11.5	69.2	15.4	0.0	0.0
135.0	0.0	0.0	0.0	0.0	0.0	0.0	0.0	0.0	0.0	0.0	0.0	0.0	30.0	65.0	5.0	0.0
157.5	0.0	0.0	0.0	0.0	0.0	0.0	8.0	0.0	0.0	0.0	0.0	0.0	0.0	0.0	84.0	8.0
180.0	8.0	0.0	0.0	0.0	0.0	0.0	2.0	0.0	0.0	0.0	0.0	0.0	2.0	0.0	24.0	64.0

Estimated Orientation [deg]

(b) **Nearest Neighbor**

True Orientation [deg]	-157.5	-135.0	-112.5	-90.0	-67.5	-45.0	-22.5	-0.0	22.5	45.0	67.5	90.0	112.5	135.0	157.5	180.0
-157.5	89.7	7.7	0.0	0.0	0.0	0.0	0.0	0.0	0.0	0.0	0.0	0.0	0.0	0.0	0.0	2.6
-135.0	16.0	60.0	24.0	0.0	0.0	0.0	0.0	0.0	0.0	0.0	0.0	0.0	0.0	0.0	0.0	0.0
-112.5	0.0	3.6	85.7	7.1	3.6	0.0	0.0	0.0	0.0	0.0	0.0	0.0	0.0	0.0	0.0	0.0
-90.0	0.0	0.0	15.4	61.5	23.1	0.0	0.0	0.0	0.0	0.0	0.0	0.0	0.0	0.0	0.0	0.0
-67.5	0.0	0.0	5.6	11.1	83.3	0.0	0.0	0.0	0.0	0.0	0.0	0.0	0.0	0.0	0.0	0.0
-45.0	0.0	0.0	7.1	0.0	28.6	50.0	14.3	0.0	0.0	0.0	0.0	0.0	0.0	0.0	0.0	0.0
-22.5	0.0	5.3	5.3	0.0	0.0	0.0	78.9	5.3	0.0	0.0	0.0	0.0	0.0	0.0	5.3	0.0
-0.0	2.0	2.0	0.0	0.0	0.0	0.0	2.0	88.0	4.0	0.0	0.0	0.0	0.0	0.0	0.0	2.0
22.5	0.0	0.0	0.0	0.0	0.0	0.0	0.0	16.3	75.5	8.2	0.0	0.0	0.0	0.0	0.0	0.0
45.0	0.0	0.0	0.0	0.0	0.0	0.0	0.0	2.6	5.1	76.9	15.4	0.0	0.0	0.0	0.0	0.0
67.5	0.0	0.0	0.0	0.0	0.0	0.0	0.0	0.0	0.0	16.0	76.0	8.0	0.0	0.0	0.0	0.0
90.0	0.0	0.0	0.0	0.0	0.0	0.0	0.0	0.0	0.0	0.0	25.0	60.0	15.0	0.0	0.0	0.0
112.5	3.8	0.0	0.0	0.0	0.0	0.0	0.0	0.0	0.0	0.0	0.0	7.7	76.9	11.5	0.0	0.0
135.0	0.0	0.0	0.0	0.0	0.0	0.0	0.0	0.0	0.0	0.0	0.0	0.0	25.0	60.0	15.0	0.0
157.5	0.0	2.0	0.0	0.0	0.0	0.0	0.0	0.0	0.0	0.0	0.0	0.0	0.0	0.0	94.0	4.0
180.0	4.0	0.0	0.0	0.0	0.0	0.0	0.0	4.0	0.0	0.0	0.0	0.0	0.0	0.0	6.0	86.0

Estimated Orientation [deg]

(c) **Support Vector Machine [6]**

True Orientation [deg]	-157.5	-135.0	-112.5	-90.0	-67.5	-45.0	-22.5	-0.0	22.5	45.0	67.5	90.0	112.5	135.0	157.5	180.0
-157.5	82.1	7.7	0.0	0.0	0.0	0.0	0.0	5.1	5.1	0.0	0.0	0.0	0.0	0.0	0.0	0.0
-135.0	20.0	32.0	20.0	0.0	0.0	0.0	0.0	0.0	0.0	16.0	0.0	0.0	0.0	0.0	12.0	0.0
-112.5	0.0	0.0	82.1	3.6	3.6	0.0	0.0	0.0	0.0	0.0	0.0	0.0	0.0	0.0	10.7	0.0
-90.0	0.0	0.0	30.8	38.5	23.1	0.0	0.0	0.0	0.0	0.0	0.0	0.0	0.0	0.0	0.0	7.7
-67.5	0.0	0.0	11.1	16.7	55.6	5.6	0.0	5.6	0.0	0.0	0.0	0.0	0.0	5.6	0.0	0.0
-45.0	21.4	0.0	14.3	0.0	28.6	14.3	7.1	0.0	0.0	0.0	0.0	0.0	0.0	7.1	7.1	0.0
-22.5	5.3	0.0	5.3	0.0	0.0	0.0	15.8	5.3	0.0	0.0	0.0	0.0	0.0	0.0	57.9	10.5
-0.0	0.0	0.0	0.0	0.0	0.0	0.0	2.0	90.0	6.0	2.0	0.0	0.0	0.0	0.0	0.0	0.0
22.5	2.0	0.0	0.0	0.0	0.0	0.0	0.0	14.3	77.6	6.1	0.0	0.0	0.0	0.0	0.0	0.0
45.0	0.0	0.0	0.0	0.0	0.0	0.0	0.0	2.6	5.1	82.1	7.7	0.0	0.0	0.0	2.6	0.0
67.5	0.0	0.0	0.0	0.0	0.0	0.0	0.0	0.0	0.0	20.0	68.0	8.0	4.0	0.0	0.0	0.0
90.0	0.0	0.0	0.0	0.0	0.0	0.0	0.0	5.0	0.0	0.0	25.0	40.0	25.0	0.0	0.0	5.0
112.5	0.0	0.0	0.0	0.0	0.0	0.0	0.0	0.0	0.0	0.0	0.0	3.8	84.6	3.8	7.7	0.0
135.0	0.0	0.0	0.0	0.0	0.0	0.0	0.0	0.0	40.0	0.0	0.0	0.0	10.0	25.0	25.0	0.0
157.5	0.0	0.0	0.0	0.0	0.0	0.0	0.0	0.0	0.0	0.0	0.0	0.0	0.0	0.0	94.0	6.0
180.0	6.0	0.0	0.0	0.0	0.0	0.0	0.0	8.0	0.0	0.0	0.0	0.0	0.0	0.0	10.0	76.0

Estimated Orientation [deg]

(d) **Random Jungle [14]**

Figure 21. **Confusion Matrices of Orientation Classification using Histogram of Oriented Gradients as Features**

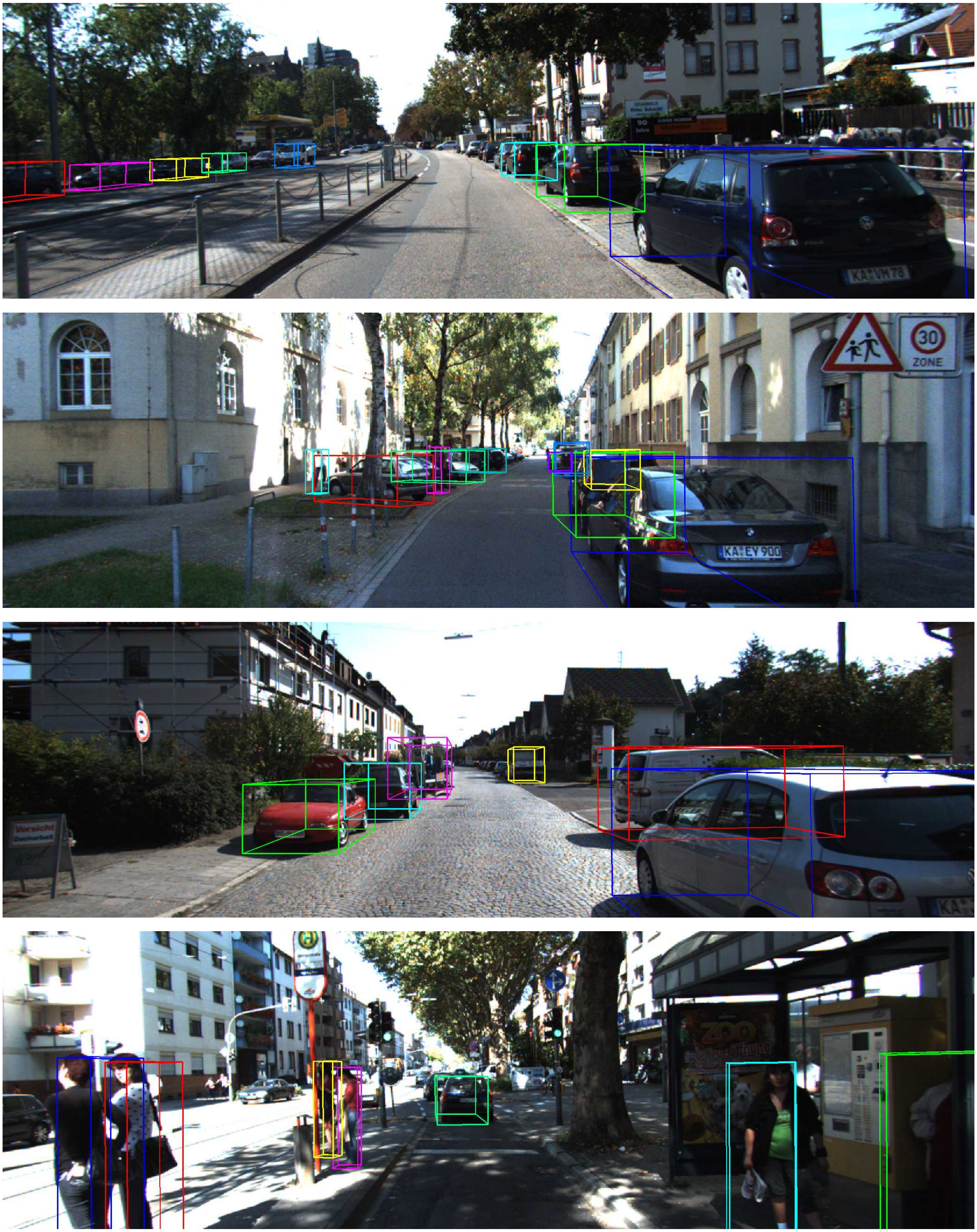

Figure 22. **3D Object: Sample Scenes from our Dataset**

CVPR #954

Figure 23. **3D Object: Sample Scenes from our Dataset**

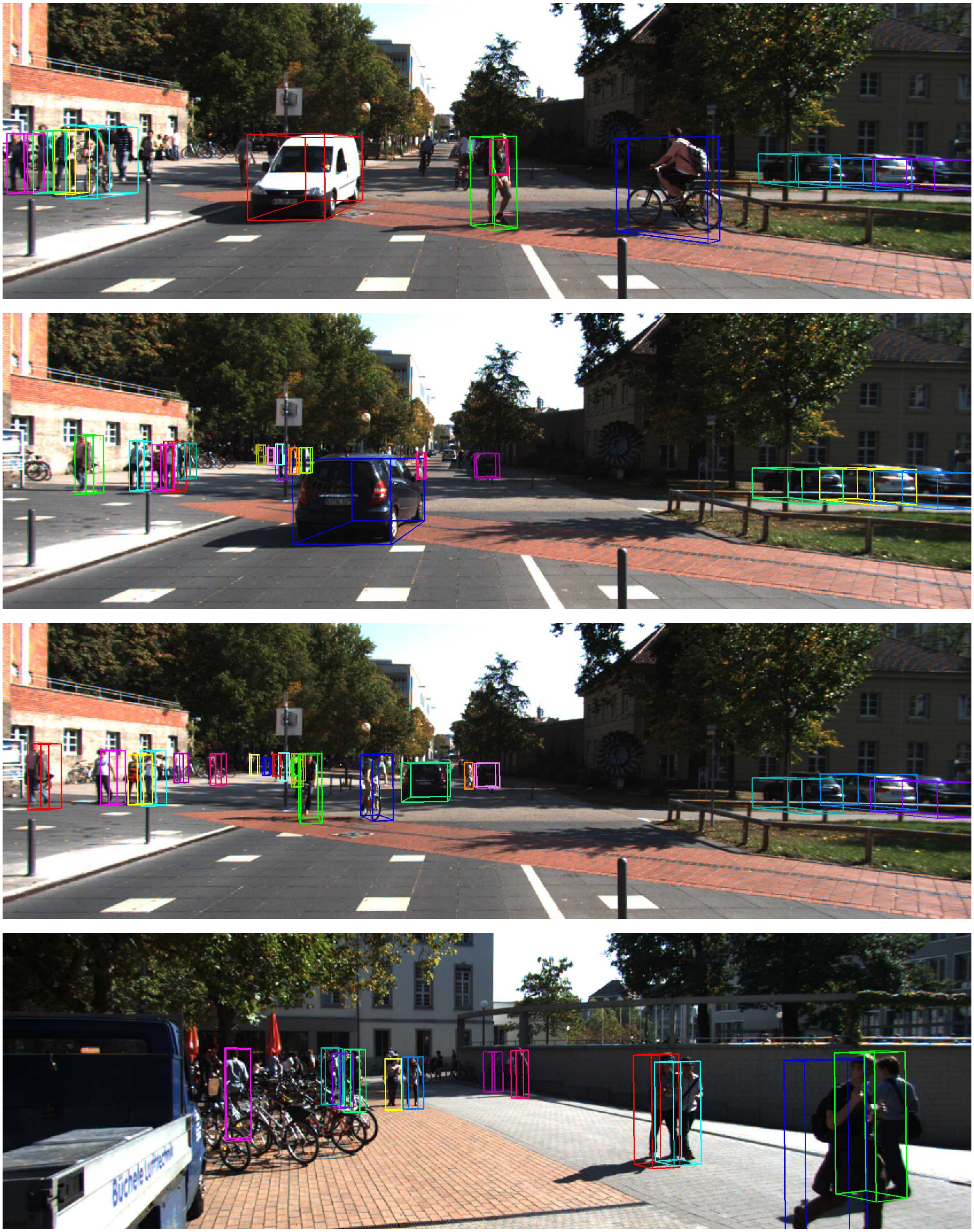

Figure 24. **3D Object: Sample Scenes from our Dataset**

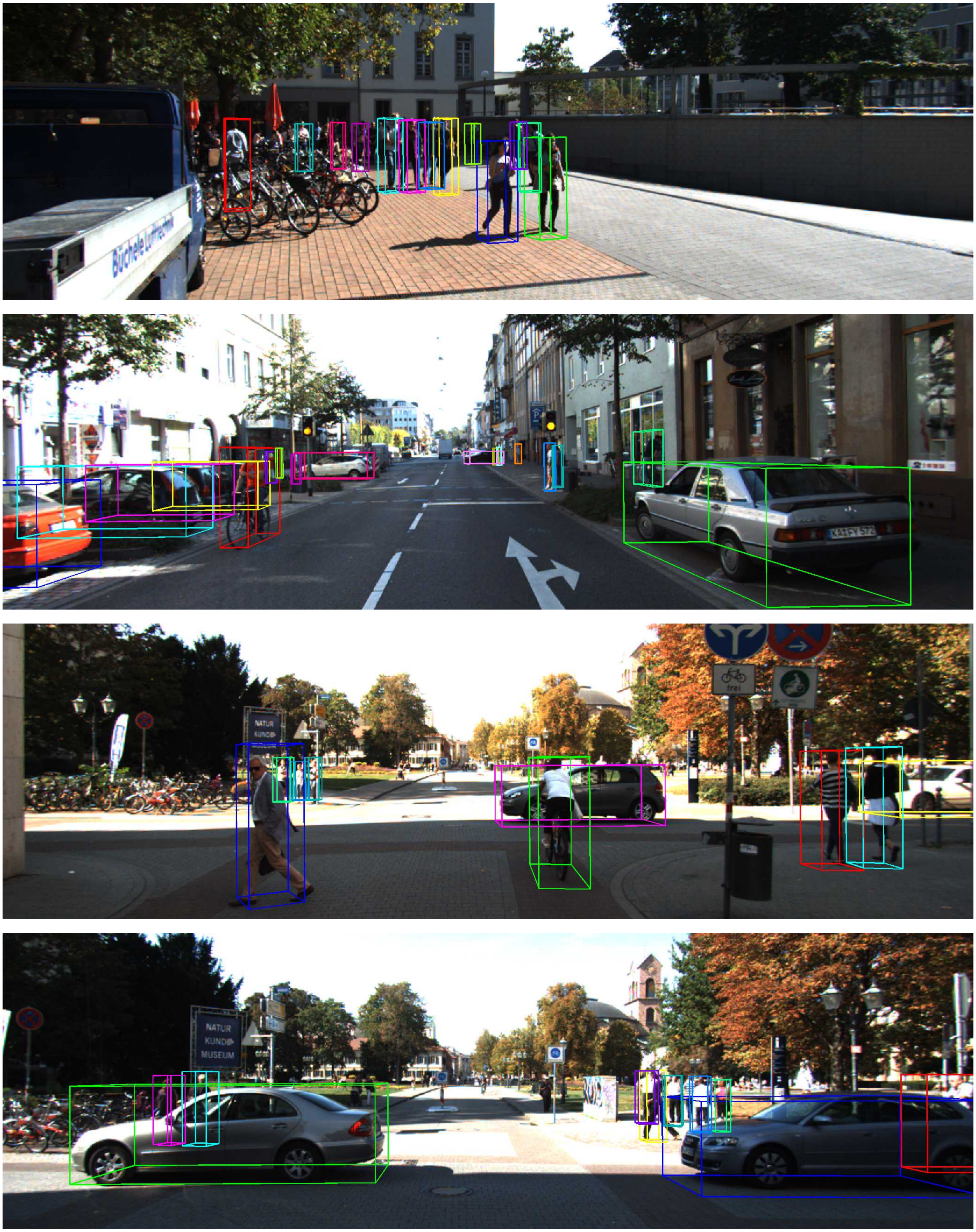

Figure 25. **3D Object: Sample Scenes from our Dataset**

References

[1] G. Bradski. The opencv library. *Dr. Dobb's Journal of Software Tools*, 2000. 2, 3

[2] T. Brox, A. Bruhn, N. Papenberg, and J. Weickert. High accuracy optical flow estimation based on a theory for warping. In *ECCV*, 2004. 2, 3

[3] T. Brox and J. Malik. Large displacement optical flow: Descriptor matching in variational motion estimation. *PAMI*, 33:500–513, March 2011. 2, 3

[4] J. Cech, J. Sanchez-Riera, and R. P. Horaud. Scene flow estimation by growing correspondence seeds. In *CVPR*, 2011. 2, 3

[5] J. Cech and R. Sara. Efficient sampling of disparity space for fast and accurate matching. In *BenCOS*, 2007. 2, 3

[6] C.-C. Chang and C.-J. Lin. Libsvm: a library for support vector machines. Technical report, 2001. 24

[7] A. Geiger, M. Roser, and R. Urtasun. Efficient large-scale stereo matching. In *ACCV*, 2010. 2, 3

[8] H. Hirschmueller. Stereo processing by semiglobal matching and mutual information. *PAMI*, 30:328–41, 2008. 2, 3

[9] B. K. P. Horn and B. G. Schunck. Determining optical flow: A retrospective. *AI*, 59:81–87, 1993. 2, 3

[10] V. Kolmogorov and R. Zabih. Computing visual correspondence with occlusions using graph cuts. In *ICCV*, pages 508–515, 2001. 2, 3

[11] J. Kostkova. Stratified dense matching for stereopsis in complex scenes. In *BMVC*, 2003. 2, 3

[12] C. Rhemann, A. Hosni, M. Bleyer, C. Rother, and M. Gelautz. Fast cost-volume filtering for visual correspondence and beyond. In *CVPR*, 2011. 2, 3

[13] S. Rusinkiewicz and M. Levoy. Efficient variants of the icp algorithm. In *3DIM*, June 2001.

[14] D. Schwarz, I. König, and A. Ziegler. On safari to random jungle: a fast implementation of random forests for high-dimensional data. *Bioinformatics*, 27:439, 2011. 24

[15] D. Sun, S. Roth, and M. J. Black. Secrets of optical flow estimation and their principles. In *CVPR*, 2010. 2, 3

[16] J. yves Bouguet. Pyramidal implementation of the lucas kanade feature tracker. *Intel*, 2000. 2, 3

[17] C. Zach, T. Pock, and H. Bischof. A duality based approach for realtime tv-l1 optical flow. In *DAGM*, pages 214–223, 2007. 2, 3